Published in : Matrix Biology (2018), vol. 70, pp. 140–157
DOI: https://doi.org/10.1016/j.matbio.2018.04.002
Status : Postprint (Author's version)

SPONTANEOUS ATOPIC DERMATITIS DUE TO IMMUNE DYSREGULATION IN MICE LACKING ADAMTS2 AND 14

L. Dupont [a], G. Ehx [b], M. Chantry [a], C. Monseur [a], C. Leduc [a], L. Janssen [a], D. Cataldo [c], M. Thiry [d], C. Jerome [e], J.-M. Thomassin [e], B. Nusgens [a], J. Dubail [a,f], F. Baron [b] and A. Colige [a]

[a] - *Laboratory of Connective Tissues Biology, GIGA-R, University of Liege, 4000 Sart Tilman, Belgium*
[b] - *Laboratory of Hematology, GIGA-R, University of Liege, 4000 Sart Tilman, Belgium*
[c] - *Laboratory of Tumor and Developmental Biology, GIGA-R, University of Liege, 4000 Sart Tilman, Belgium*
[d] - *Laboratory of Cell Biology, GIGA-R, University of Liege, 4000 Sart Tilman, Belgium*
[e] - *Center for Educational and Research on Macromolecules (CERM), University of Liege, 4000 Sart Tilman, Belgium*
[f] - *Department of Genetics, INSERM UMR1163, Institut Imagine, Paris, France*

KEYWORDS : ADAMTS ; Collagen ; Skin ; Dermatitis ; Immunity

ABBREVIATIONS USED : WT, wild type mice ; TS2$^{-/-}$, Adamts2-deficient mice ; TS14$^{-/-}$, Adamts14-deficient mice ; TS2$^{-/-}$/TS14$^{-/-}$, Adamts2-Adamts14-deficient mice.

ABSTRACT :

Since its first description, ADAMTS14 has been considered as an aminoprocollagen peptidase based on its high similarity with ADAMTS3 and ADAMTS2. As its importance for procollagen processing was never experimentally demonstrated *in vivo*, we generated *Adamts14*-deficient mice. They are healthy, fertile and display normal aminoprocollagen processing. They were further crossed with *Adamts2*-deficient mice to evaluate potential functional redundancies between these two highly related enzymes. Initial characterizations made on young *Adamts2-Adamts14*-deficient animals showed the same phenotype as that of Adamts2- deficient mice, with no further reduction of procollagen processing and no significant aggravation of the structural alterations of collagen fibrils. However, when evaluated at older age, *Adamts2-Adamts14*-deficient mice surprisingly displayed epidermal lesions, appearing in 2 month-old males and later in some females, and then worsening rapidly. Immunohistological evaluations of skin sections around the lesions revealed thickening of the epidermis, hypercellularity in the dermis and extensive infiltration by immune cells. Additional investigations, performed on young mice before the formation of the initial lesions, revealed that the primary cause of the phenotype was not related to alterations of the epidermal barrier but was rather the result of an abnormal activation and differentiation of T lymphocytes towards a Th1 profile. However, the primary molecular defect probably does not reside in the immune system itself since irradiated *Adamts2-Adamts14*-deficient mice grafted with WT immune cells still developed lesions.

While originally created to better characterize the common and specific functions of ADAMTS2 and ADAMTS14 in extracellular matrix and connective tissues homeostasis, the *Adamts2-Adamts14*-deficient mice revealed an unexpected but significant role of ADAMTS in the regulation of immune system, possibly through a cross-talk involving mesenchymal cells and the TGFβ pathways.

Published in : Matrix Biology (2018), vol. 70, pp. 140–157
DOI: https://doi.org/10.1016/j.matbio.2018.04.002
Status : Postprint (Author's version)

Introduction

Together with MMPs (Matrix Metalloproteinase), ADAMs (A Disintegrin And Metalloproteinase) and Astacins, ADAMTS (A Disintegrin And Metalloproteinase with ThromboSpondin type I repeat) are zinc-dependent metalloproteinases active in the extracellular space [1]. They form a family of 19 members possessing an identical N-terminal domain composi-tion, including the metalloproteinase domain and one thrombospondin type 1 repeat (TSR1) [2]. Human genetic diseases and spontaneous or engineered mutations in rodent underline the diversity of their functions, their critical roles in various physio-pathological conditions and the existence of redundancies between the closest ADAMTS relatives [3]. Subfamilies have been defined based on enzyme activity and composition of the C-terminal ancillary domains. ADAMTS2, 3 and 14 are the only ADAMTS that possess 3 additional consecutive TSR1 followed by a short C-terminal domain containing a PLAC (Protease and Lacunin) signature [2]. The cleavage of the amino- and carboxy-propeptides of fibrillar procollagens is required for the assembly of collagen trimers into well-organized fibrils and fibers. The carboxy-propeptide domain is cleaved by BMP1/ Tolloid like metalloproteinases [4,5] and ADAMTS2 (previously known as "aminoprocollagen peptidase" or "procollagen *N*-proteinase") was the first enzyme described for its capacity to excise the aminopropeptide of fibrillar collagens [6–9]. Later, ADAMTS3 was found to be responsible for the processing of the aminopropeptide of type II procollagen in cartilage [10]. Mutations preventing the expression of active ADAMTS2 lead to the dermatosparactic type of Ehlers-Danlos syndrome in human, and to similar pathologic features in several animal species [11,12]. *Adamts2*-deficient mice, similarly to human patients and affected animals, are mainly characterized by severe skin fragility and variable, but milder, alterations of other connective tissues [13]. These phenotypic changes have been linked to the accumulation of aminoprocollagen I (type I collagen still retaining its aminoterminal propeptide) which results in the formation of abnormal collagen fibers displaying reduced mechanical resistance. It is worth noting also that, despite the constitutive absence of ADAMTS2 activity in dermatosparaxis, a significant proportion of type I collagen is correctly processed, even in the skin, and that the proportion of aminoprocollagen I strongly varies from one tissue to another [14–16]. These observations suggested the existence of functional redundancies between these three related ADAMTS. Absence of Adamts3 is embryonically lethal at 15 days post coitum [17]. The processing of fibrillar collagens is however not altered in these embryos. Instead, it was demonstrated that Adamts3 is required for the development of the lymphatic network by its capacity to cleave pro-VEGF-C into active VEGF-C capable to trigger the VEGF-R3 pathway [17,18]. Furthermore, we recently showed that loss of ADAMTS3 activity in human causes Hennekam lymphangiectasia-lymphedema syndrome 3 by a lack of proteolytic activation of pro-VEGFC [19]. ADAMTS14 has remained much less characterized. In addition to a low aminoprocollagen peptidase activity measured *in vitro* [14], genetic linkage has been found with multiple sclerosis [20] and osteoarthritis [21], two conditions that probably do not directly involve the processing of newly synthesized procollagens. Other studies linking ADAMTS2 to angiogenesis [22], inflammation [23] and cardiovascular diseases [24,25] similarly indicate that the collective functions of ADAMTS2, 3 and 14 are not restricted to collagen biology. The aim of the present study was to elucidate the physiological roles of ADAMTS14 through *Adamts14* gene

Published in : Matrix Biology (2018), vol. 70, pp. 140–157
DOI: https://doi.org/10.1016/j.matbio.2018.04.002
Status : Postprint (Author's version)

inactivation in mice and to determine its potential redundancy with Adamts2 by creating *Adamts2* and *Adamts14* doubly deficient mice.

Material and methods

GENERATION OF ADAMTS14-DEFICIENT MICE AND ADAMTS2-ADAMTS14 DOUBLY DEFICIENT MICE

Embryonic stem (ES) cells were engineered at the Centre for Modeling Human Disease (Toronto, Canada) and mosaic and heterozygous mice were generated at the Transgenic Core Facility of the Toronto Centre for Phenogenomics (Toronto, Canada). R1 ES cells were transduced with a UPA gene trap vector (Figure S1) [26] and then selected for neomycin-resistance with Geneticin (G418). RNA from subclones were used to generate cDNA that were amplified by 3′RACE PCR. Insertion sites of gene trap cassettes were then determined by sequencing of the 3′RACE products. One clone (CMHD-GT_511E11) was positive for an insertion between bases 9251 and 9252 of intron 4 of the *Adamts14* gene. Cells of this clone were then fused to C57bl/6 blastocysts to obtain mosaic mice that were further used to obtain heterozygous founders. The heterozygous mice were finally intercrossed to obtain homozygous mice. Genotyping of tail DNA was performed using the following primers: P1 (5′-TTAATGGCTCACTCCCCACTGAAC-3′) and P2 (5′-TTCCTTGGGAGGGTCTCCTCTGA-3′) for amplifying the targeted allele while P1 and P3 (5′-GCCA GGAAGGACCAGTGATCCTC-3′) were used for the wild type allele (Figure S1).

Adamts14 expression was evaluated on RNA purified (Nucleospin RNA/protein kit, Macherey/ Nagel, Germany) from skin of wild type (WT), heterozygous ($TS14^{+/-}$) and homozygous ($TS14^{-/-}$) mice. RT-PCR amplifications were performed using Tth DNA Polymerase (Roche, Bâle, Switzerland) and pairs of primers allowing the amplification of different sequences (exons 4 to 6 [forward: 5′-ACTACGTGCT GACGCTCATGAATAT-3′; reverse 5′-GCCCAGC GACACACCTGCTCCA-3′], exons 2 to 3 [forward: 5′-TGTACACTGGAGGTGTCACTGGAA-3′; reverse: 5′-TGGTGAAGGTCACCATGAGGCTCT-3′], exons 5 to 7 [forward 5′-CTGATCATGGTGGGCTACCGACA- 3′; reverse 5′-CCATCCTCGTGGTTGAGGGCACA- 3′] of *Adamts14*; GFP [forward 5′-CACATGAAGCAG CACGACTTCTTC-3′; reverse 5′-GGCGGATCT TGAAGT TCACCTTGA-3′]), in order to confirm the efficacy of the "gene trap" strategy.

For the initial characterizations, WT, $TS14^{+/-}$ and $TS14^{-/-}$ mice were generated by mating $TS14^{+/-}$ males and females. Mice doubly deficient for *Adamts2* and *Adamts14* ($TS2^{-/-}/TS14^{-/-}$) were produced by mating $TS2^{+/-}/TS14^{-/-}$ males and females. Frequent backcrosses in wildtype C57bl/6 and intercrosses between the $TS2^{+/-}$ and the $TS14^{-/-}$ genotypes were performed to insure a homogeneous genetic background.

Mice were maintained under standard laboratory conditions, with 12 hour light/12 hour dark cycles and free access to food and water. All the procedures were performed in accordance with the guidelines for animal care of the University of Liège, the Federation of European Laboratory Animal Science Associations and the American National Institutes of Health.

Published in : Matrix Biology (2018), vol. 70, pp. 140–157
DOI: https://doi.org/10.1016/j.matbio.2018.04.002
Status : Postprint (Author's version)

MECHANICAL PROPERTIES OF THE SKIN

Mechanical properties of the skin were determined using the "Instron" apparatus (Instron 5566 UTM, Instron). Six 8 week-old mice of each genotype (WT, TS14$^{-/-}$, TS2$^{-/-}$, TS2$^{-/-}$/TS14$^{-/-}$) were sacrificed and three strips of dorsal skin (1 cm width; 3 cm in length in the head to tail orientation) were excised for each mouse and fixed between the two clamps of the apparatus (distant by 1 cm). Skin strips were stretched (at 1 mm/s) until rupture. The maximal tensile strength (the maximal force in newton divided by the initial cross sectional area of the specimen) and deformation (% of elongation at rupture) were measured. The statistical significance of the differences between two genotypes was determined by Student's *t*-test.

TYPE I COLLAGEN PROCESSING

Skin, cornea and tendon were dissected, ground at liquid nitrogen temperature, homogenized in Laemmli denaturation buffer (with 100 mM DTT) and denatured (95 °C, 5 min). After electrophoresis (7.5% SDS-PAGE), the gels were stained with Coomassie blue and scanned using an ImageQuant LAS4000 device and software (GE Healthcare).

TRANSMISSION ELECTRON MICROSCOPY

Skin and tendon samples were washed in Sörensen buffer, fixed in 2.5% glutaraldehyde in a 0.1 mol/L Sörensen phosphate buffer (pH 7.4), postfixed in 1% osmium tetroxide and embedded in Epon. Ultrathin sections were contrasted with uranyl acetate and lead citrate. Observations were made with a JEM 1400 TEM.

IMMUNOHISTOLOGICAL ANALYSES

Skin samples were fixed in a 4% paraformaldehyde (PFA) solution in PBS. Paraffin-embedded tissue sections (5 µm) were deparaffined and rehydrated.

Tissue sections were stained with hematoxylin/eosin for general histology or with toluidine blue to assess mast cells infiltration. Immunohistological staining of skin sections was performed using Ki67 (Dako, Glostrup, Denmark), cytokeratin 10 (Novus Biologicals, Littleton, USA), CD45 (BD Biosciences, Allschwil, Suisse), CD3 (Roche, Bâle, Suisse), interferon gamma (Bioss, Woburn, USA) and cleaved caspase 3 (Cell Signaling, Danvers, USA) antibodies.

IN SITU HYBRIDIZATION

For specificity reasons the design of the probes was made in regions encompassing several exons and with the lowest homologies between *Adamts2*, 3 and 14 (Table S1). Amplification of these sequences were performed using the forward or the reverse primer (in bold) starting by the T7 RNA polymerase promoter sequence to generate antisense or sense probes. The purified cDNAs were used to generate antisense and sense cRNA probes using a T7 DIG RNA labeling kit (Roche) and digoxigenin-11-UTP (Roche) according to the manufacturer's specifications. Paraffin sections of

Published in : Matrix Biology (2018), vol. 70, pp. 140–157
DOI: https://doi.org/10.1016/j.matbio.2018.04.002
Status : Postprint (Author's version)

paraformaldehyde-fixed samples (newborns and 8 week-old wild-type mouse skin) were hybridized to 10 µg/mL DIG-11-UTP-labeled *Adamts2* or *Adamts14* cRNA probes as previously described [27]. After staining in the dark with 5-bromo-4-chloro-3'-indoylphosphate *p*-toluidine salt (BCIP) and nitroblue tetrazolium chloride (NBT) (Roche) according to manufacturer's recommendations, slides were scanned using a Nanozoomer 2.0 scanner (Hamamatsu) and visualized using NDPviewer (Hamamatsu).

INDUCTION OF LOCAL SKIN INFLAMMATION BY TOPICAL APPLICATION OF IMIQUIMOD

A daily topical dose of 62.5 mg of commercially available Imiquimod cream (5%) (Aldara Cream; Meda AB, Solna, Sweden) was applied to the shaved back skin and ears of 8 week-old mice for 5 consecutive days. Mice were killed 3 days after the last application and skin was fixed in 4% PFA for immunohistological analysis.

MEASUREMENT OF TRANSEPIDERMAL WATER LOSS

A Courage and Khazaka Tewameter TM210 (CK Technology SPRL, Visé, Belgium) was used for measuring transepidermal water loss (TEWL) on the dorsal flank and on belly of 6 mice per genotype 24 h after hair shaving. TEWL was recorded at ambient temperature (19 °C to 21 °C) and humidity (50% ± 5%).

FLOW CYTOMETRY

At the time of sacrifice, peripheral blood and spleen were collected and analyzed by flow cytometry. Splenocytes were obtained by crushing the spleen. Cells were counted with an ABX Micros 60 (HORIBA Medical). Peripheral blood was depleted of erythro-cytes using RBC lysis buffer (eBioscience, San-Diego, CA, USA) according to manufacturer's instructions. The following antibodies were used: anti-CD45-PerCPCy5.5 (30-F11), anti-CD3-PE (145-2C11, Becton-Dickinson (BD), Bedford, MA, USA), anti-CD3-V500 (500A2, BD), anti-CD11b-APC (M1/70), anti-Gr-1-V450 (RB6-8C5), anti-B220-APC-eFluor780 (RA3-6B2), anti-CD4-BV510 (RM4-5, SONY Biotechnology, The Heights, Surrey, UK), anti-CD4-eFluor450 (RM4-5), anti-CD8-PECy7 (53-6.5), anti-CD8-PerCPCy5.5 (53-6.5), anti-CD8-APC-eFluor780 (536.5), anti-CD25-PECy7 (PC61, BD), anti-ICOS-BV421 (7E.17G9, BD), anti-CD44-FITC (IM7), anti-CD62L-APC-eFluor780 (MEL-14), anti-CD49b-biotin (DX5), anti-FoxP3-PE (FJK-16s), anti-Ki67-AlexaFluor647 (B56, BD), anti-IFNγ-PerCPCy5.5 (XMG1.2), anti-IL-4-PECy7 (BVD6-24G2), anti-IL-17-APC (eBio17B7) and anti-IL-2-PE (JES6-5H4) (all from eBioscience unless otherwise indicated). Cells (1.5-2 × 10^6 cells/ sample) were incubated with antibodies for 20 min at 4 °C in the dark and washed twice with PBS/3% FBS (Lonza, Verviers, Belgium). Intracellular staining for FoxP3, KI67 and cytokines was performed by using the FoxP3 Staining Buffer Set (eBioscience). For intracellular cytokine staining, spleen homogenates were stimulated for 4 h in RPMI supplemented with 10% FBS, penicillin (100 U/mL) and streptomycin (10 mg/mL) by PMA/ionomycin, brefeldin A and monensin (Cell Stimulation Cocktail + Protein Transport Inhibitors,

Published in : Matrix Biology (2018), vol. 70, pp. 140–157
DOI: https://doi.org/10.1016/j.matbio.2018.04.002
Status : Postprint (Author's version)

eBioscience). Absolute counts were performed with TruCount tubes (BD). Data were acquired on a FACS Canto II flow cytometer (Becton Dickinson) and analyzed with the Flowjo software 7.0 (Tree Star Inc., Ashland, OR). The Mann-Whitney *U* test was used to compare data between experimental groups.

REGULATORY T CELLS SUPPRESSION ASSAY

Regulatory T cells (Treg, $CD3^+CD4^+CD25^+$) and conventional T cells (Tconv, $CD3^+CD4^+CD25^-$) were sorted by flow cytometry (FACS Aria III, Becton-Dickinson) from spleens harvested from mice sacrificed at the age of 12 weeks. Tconvs were labeled with CFSE (carboxyfluorescein diacetate succinimidyl ester) at 5 µM and were cultured in RPMI supplemented with 10% FBS, in the presence of CD3/CD28 beads (Bead: Cell ratio 1:8, Dynabeads, Invitrogen). Unlabeled Tregs were mixed or not with Tconvs at different Treg:Tconv ratio, in triplicate. Cells were harvested from culture after 72 h, stained with 7-AAD (7-aminoactinomycin D), and analyzed by flow cytometry (FACS Canto II). The suppressive capacity of Tregs was expressed as the relative inhibition of the percentage of $(CFSE)^{low}$ Tconvs (100 × (1 - $\%CFSE^{low}$ Tconvs in coculture / $\%CFSE^{low}$ Tconvs alone)).

BONE MARROW TRANSPLANT

Bone marrow from femurs and tibias from six WT and six $TS2^{-/-}/TS14^{-/-}$ 8 week-old male mice was collected in sterile RPMI + 10% FBS + 1% penicillin/ streptomycin. The suspensions were passed through a70µm nylon filter mesh and washed with PBS + 3% FBS + 1% P/S. Cells were then resuspended and mixed in PBS at a concentration of 10×10^6 bone marrow cells/200 µL. Recipient mice (six WT and six $TS2^{-/-}/TS14^{-/-}$) were injected intravenously with 200 µL of the cell suspension, 6 h after having received a total body irradiation of 11Gy.

Five irradiated $TS2^{-/-}/TS14^{-/-}$ were grafted with WT bone marrow and one with $TS2^{-/-}/TS14^{-/-}$ bone marrow, as control. An identical experimental design was used for the six irradiated WT mice (5 grafted with $TS2^{-/-}$ /$TS14^{-/-}$ bone marrow and 1 with WT bone marrow).

Results

ADAMTS14 INACTIVATION HAS NO OBVIOUS PHENOTYPICAL CONSEQUENCE

Heterozygous $TS14^{+/-}$ obtained from the F1 generation were crossed to generate $TS14^{-/-}$ mice. Examination of different litters from $TS14^{+/-}$ mice mating showed a Mendelian ratio among wild type, heterozygous and homozygous deficient mice. RT-PCR were performed using different pairs of primers on mRNA extracted from skin of WT, $TS14^{+/-}$ and $TS14^{-/-}$ mice. Primers located on either side of the cassette (exon 4–exon 6) allowed the amplification of RT-PCR products from WT and $TS14^{+/-}$ but not from $TS14^{-/-}$ mRNA demonstrating the efficacy of the trapping mechanism (Figure S2). As an additional control, GFP was amplified only from $TS14^{+/-}$ and $TS14^{-/-}$ mice as expected in case of

Published in : Matrix Biology (2018), vol. 70, pp. 140–157
DOI: https://doi.org/10.1016/j.matbio.2018.04.002
Status : Postprint (Author's version)

successful integration of the cassette. Finally, primers specific for regions located upstream (exons 2–3) or downstream (exons 5–7) of the cassette generated RT-PCR products for the three genotypes. Altogether these data illustrate the existence of two individual transcripts when the cassette is inserted in the intron 4 of *Adamts14*, clearly demonstrating the efficacy of the trapping mechanism (Figure S2).

Adult TS14$^{-/-}$ males and females were fertile and their mating produced the expected Mendelian ratio. Fibrillar collagen processing was evaluated in tissues characterized by a high collagen content (tendon, skin and cornea). The electrophoretic pattern of collagen chains was identical in wild type and TS14$^{-/-}$ mice (Figure 1), suggesting that ADAMTS14 does not possess significant aminoprocollagen peptidase activity *in vivo* or that this activity can be seen only in situations where ADAMTS2 activity is absent.

Figure 1. *Type I procollagen processing. Skin, tendon and cornea samples from three mice of each genotype were homogenized and extracted in Laemmli denaturation buffer containing DTT. Proteins corresponding to an identical amount of tissue were submitted to SDS-PAGE and stained (Coomassie blue). In tissues from WT and TS14$^{-/-}$ mice, type I collagen appeared as two bands corresponding to the fully processed alpha1 (α1I) and alpha2 (α2I) chains. Two additional bands corresponding to alpha1 and alpha2 chains still retaining their aminopropeptide (pNα1I and pNα2I, respectively) were observed in the tissues of mice lacking Adamts2 activity (TS2$^{-/-}$ and TS2$^{-/-}$/TS14$^{-/-}$). The alteration of the maturation (reduction of the conversion of pNα1I and pNα2I into α1I and α2I, respectively) was more pronounced in the skin. In the three tissues, the absence of Adamts14 activity did not lead to an increased accumulation of pNα1 or pNα2 chains (compare the accumulation of pNα chains in TS2$^{-/-}$ and in TS2$^{-/-}$/TS14$^{-/-}$ mice).*

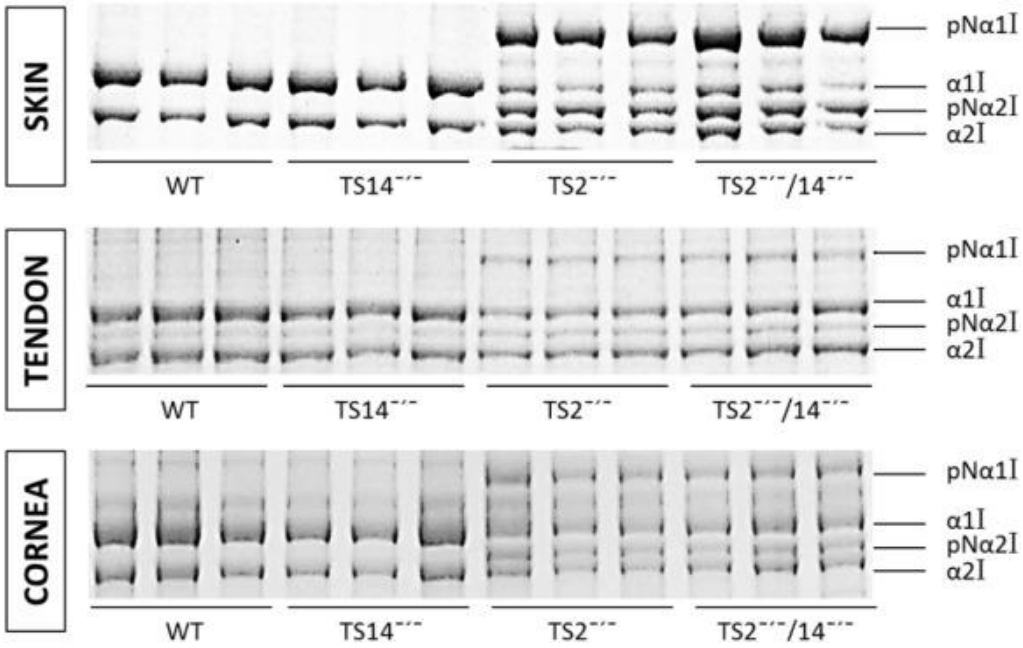

Published in : Matrix Biology (2018), vol. 70, pp. 140–157
DOI: https://doi.org/10.1016/j.matbio.2018.04.002
Status : Postprint (Author's version)

ADAMTS14 IS NOT SIGNIFICANTLY INVOLVED IN COLLAGEN FIBRILS FORMATION IN VIVO

$TS14^{+/-}$ and $TS2^{+/-}$ mice were mated and their $TS2^{+/-}/TS14^{-/-}$ progeny were used to generate doubly deficient mice ($TS2^{-/-}/TS14^{-/-}$). During the crossing process, all the expected genotypes were observed with a normal Mendelian frequency, which indicated an absence of embryonic lethality. Except for mice with a $TS2^{-/-}$ genotype ($TS2^{-/-}$ and $TS2^{-/-}/TS14^{-/-}$), all the genotypes were fertile, even the $TS2^{+/-}/TS14^{-/-}$ mice. Newborn pups of the different genotypes were undistinguishable. At 3 weeks of age, $TS2^{-/-}/TS14^{-/-}$ mice and $TS2^{-/-}$ mice were easily identified by the more ruffled appearance of their fur as compared to WT and $TS14^{-/-}$ mice. However, no increase of this phenotype was seen in $TS2^{-/-}/TS14^{-/-}$ doubly deficient mice as compared with $TS2^{-/-}$ mice. We then focused our analyses on 4 genotypes, i.e. WT, $TS2^{-/-}$, $TS14^{-/-}$ and $TS2^{-/-}/TS14^{-/-}$ mice. We first compared the electrophoretic pattern of type I collagen extracted from different tissues (Figure 1). In skin, only fully processed alpha 1 and alpha 2 chains were identified in WT and $TS14^{-/-}$ mice, while 50 to 80% of type I collagen still retains the aminopropeptide (pNα1I, pNα2I) in $TS2^{-/-}$ mice. There was no further reduction of aminopropeptide processing in $TS2^{-/-}/TS14^{-/-}$ mice, indicating that Adamts14 is not responsible for the residual aminoprocollagen peptidase activity observed in $TS2^{-/-}$ mice. Collagen patterns were also identical for $TS2^{-/-}$and $TS2^{-/-}/TS14^{-/-}$ mice in tendon and cornea, with alpha chains representing, respectively, about 75% and 60% of total type I collagen content (Figure 1). Finally, complete processing was observed in bone from all genotypes (Figure S3).

Differences in the mechanical properties of skin were also evaluated for the 4 genotypes by submitting skin strips to progressive elongation. Maximal tensile strength and percentage of elongation at rupture were determined (Figure 2). A slight and statistically nonsignificant reduction of skin tensile strength was observed in $TS14^{-/-}$ mice as compared to WT. As expected, the mechanical properties of skin were strongly impaired in $TS2^{-/-}$ mice and no worsened alteration was observed in $TS2^{-/-}/TS14^{-/-}$ (Figure 2).

Transmission electron microscopy was also used to examine the ultrastructure of collagen fibrils. In skin, their structure, diameter and distribution were similar in WT and $TS14^{-/-}$ mice, as expected (Figure 3). In $TS2^{-/-}$ skin, the shape of collagen fibrils was highly heterogeneous and strongly disrupted, ranging from fibrils with irregular contour to ribbon-like structure, sometimes branched (Figure 3). No further obvious increased disorganization could be evidenced in the skin of $TS2^{-/-}/TS14^{-/-}$ mice.

Analyses were also performed on other collagen-rich tissues. In tendon, collagen fibrils were identical in WT and $TS14^{-/-}$ mice and much less affected than in skin for $TS2^{-/-}$ and $TS2^{-/-}/TS14^{-/-}$ mice, with only some fibrils being less rounded, especially fibrils with small diameter or fibril tips (Figure 3). Surprisingly, the structure of the fibrils and their organization were normal in the corneas of the different genotypes (Figure S4) although pNα1I and pNα2I were present in $TS2^{-/-}$ and$TS2^{-/-}/TS14^{-/-}$ (Figure 1).

Published in : Matrix Biology (2018), vol. 70, pp. 140–157
DOI: https://doi.org/10.1016/j.matbio.2018.04.002
Status : Postprint (Author's version)

***Figure 2**. Mechanical properties of skin. Freshly excised skin strips from WT, TS14$^{-/-}$, TS2$^{-/-}$ and TS2$^{-/-}$/14$^{-/-}$ mice were clamped into an "Instron Testing System" and stretched to tensile failure at a constant rate of 1 mm/s. (A) Tensile strength was computed from maximal load at failure divided by the initial cross-sectional area of the specimen. (B) The maximal elongation at rupture was also determined and corresponded to the percentage of deformation of skin strips compared to their initial length (0% elongation). Eighteen strips per genotype were analyzed (3 strips per mouse, 6 age-matched mice of each genotype). ***P < 0.001.*

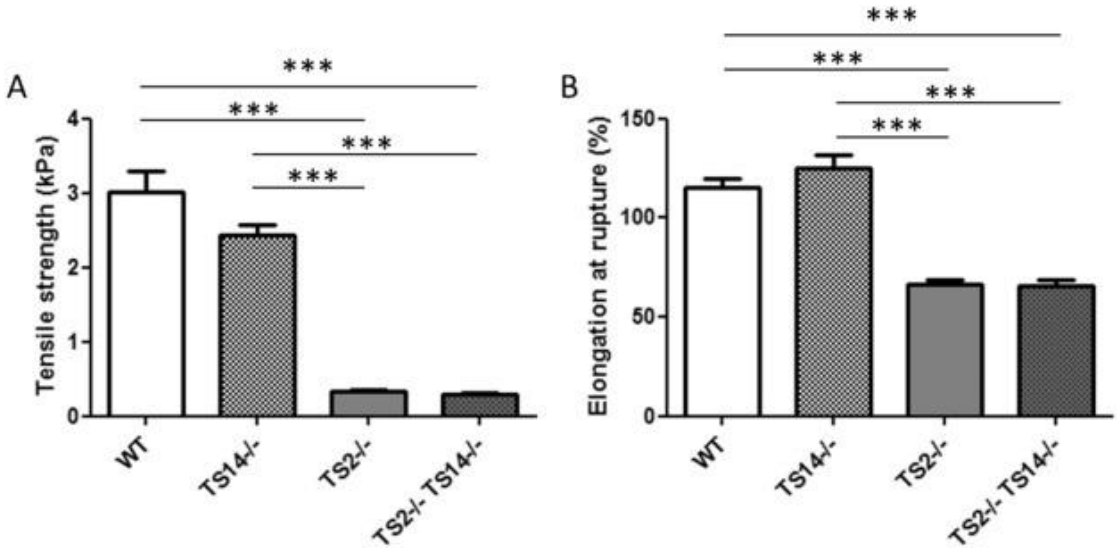

***Figure 3**. Ultrastructure of collagen fibrils in skin and tendon. In skin of WT and TS14$^{-/-}$ mice, collagen fibrils appeared cylindrical in cross section. In TS2$^{-/-}$ skin, the structure of fibrils was highly heterogeneous, ranging from fibrils with highly irregular contour to fibrils presenting "hieroglyphic" or ribbon-like structure. No aggravation of the fibril structure was noted in TS2$^{-/-}$/TS14$^{-/-}$ skin as compared to TS2$^{-/-}$. In tendons, fibrils were more closely packed than in skin, and appeared in cross section as structures with a highly variable diameter. The same general pattern was observed in WT and TS14$^{-/-}$ tendons. In TS2$^{-/-}$ and TS2$^{-/-}$/TS14$^{-/-}$ tendons, some alteration of the circular shape was observed, especially for small diameter fibrils. (Scale bar = 1 μm).*

Published in : Matrix Biology (2018), vol. 70, pp. 140–157
DOI: https://doi.org/10.1016/j.matbio.2018.04.002
Status : Postprint (Author's version)

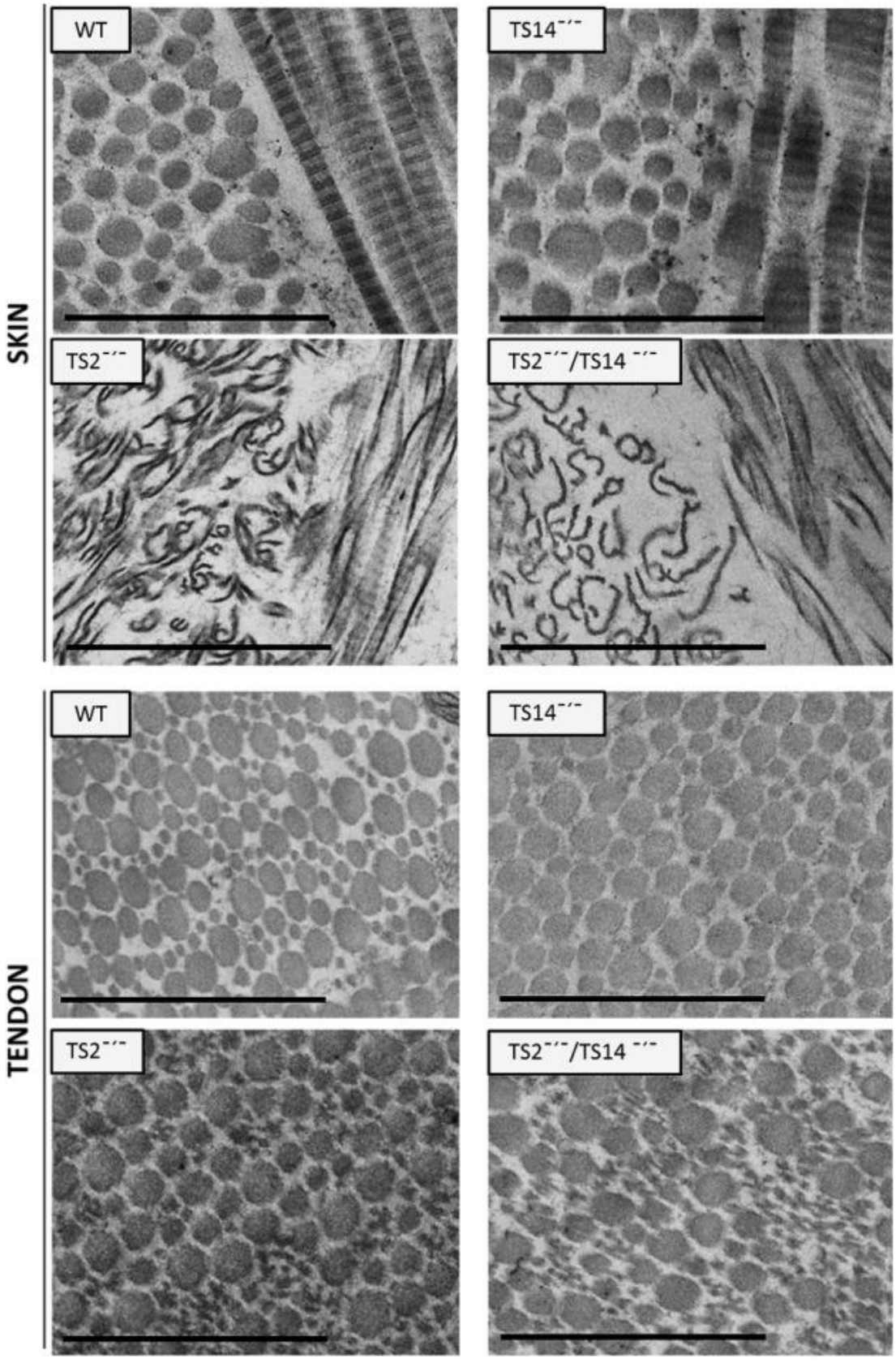

Published in : Matrix Biology (2018), vol. 70, pp. 140–157
DOI: https://doi.org/10.1016/j.matbio.2018.04.002
Status : Postprint (Author's version)

SPONTANEOUS DEVELOPMENT OF EPIDERMAL LESIONS IN TS2$^{-/-}$/TS14$^{-/-}$ ADULT MICE

All the initial characterizations of TS2$^{-/-}$/TS14$^{-/-}$ mice were made on young (≤8 weeks) animals and showed that their phenotype was identical to the phenotype of TS2$^{-/-}$ mice. At an older age, TS2$^{-/-}$/TS14$^{-/-}$ mice surprisingly started to display epidermal lesions (Figure 4A), appearing mainly in males (75% of males older than 5 months have developed lesions) (Figure 4B) and then worsening rapidly and requiring euthanasia for ethical reason.

HE staining of skin sections revealed a thickening of the epidermis and hyper-cellularity in the dermis around the lesions (Figure 5). These histological alterations tended to rapidly normalize a few mm away from the site of epidermal rupture.

Immunostaining confirmed the thickening of the epidermis (Figure 6A–D, cytokeratin 10), with a high proliferative index of the basal keratinocytes (Figure 6E–H, Ki67), infiltration by immune cells in the epidermis and the dermis (Figure 6I–L, CD45) and a moderately increased number of mastocytes (Figure 6M–P, toluidine blue) only in the affected regions of the skin of TS2$^{-/-}$/ TS14$^{-/-}$ mice.

***Figure 4**. Emergence of epidermal lesions during the aging of TS2$^{-/-}$/TS14$^{-/-}$ males. (A) Epidermal lesions appearing in TS2$^{-/-}$/TS14$^{-/-}$ mice, mainly affecting their back skin, ears, shoulders, snout and chin. (B) The earliest epidermal lesions were observed in 6 week-old TS2$^{-/-}$/TS14$^{-/-}$ mice and their frequency increased with age (n = 35, red line). Half of the mice have developed lesions by the age of 3 months. Such lesions were never observed in TS2$^{-/-}$ mice (n = 23, green line), in WT or in TS14$^{-/-}$.*

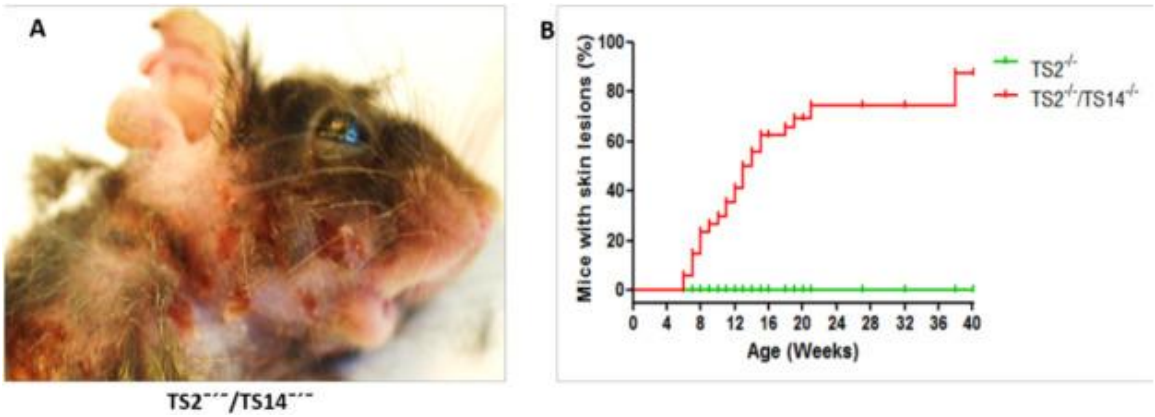

Published in : Matrix Biology (2018), vol. 70, pp. 140–157
DOI: https://doi.org/10.1016/j.matbio.2018.04.002
Status : Postprint (Author's version)

***Figure 5**. Hematoxylin-eosin staining ofWT and TS2$^{-/-}$/TS14$^{-/-}$ skin. Transversal sections of dorsal skin from WT (A) and TS2$^{-/-}$/TS14$^{-/-}$ mice with lesions (B) were stained with HE. Epidermis looked normal at some distance but progressively thickened near the lesion. The increased cellularity in the dermis was due to immune cells infiltration and to higher fibroblastic density. The number of blood vessels in the dermis was increased in TS2$^{-/-}$/TS14$^{-/-}$ mice compared with WT mice.*

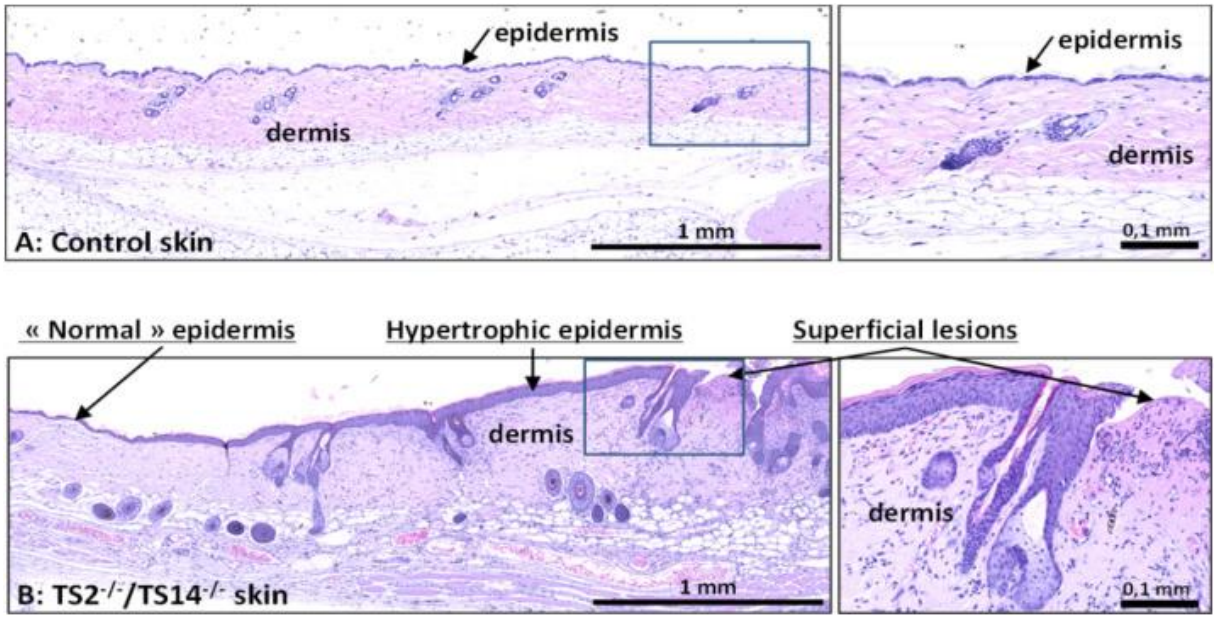

Published in : Matrix Biology (2018), vol. 70, pp. 140–157
DOI: https://doi.org/10.1016/j.matbio.2018.04.002
Status : Postprint (Author's version)

***Figure 6**. Progressive epidermal and dermal modifications in the skin of TS2$^{-/-}$/TS14$^{-/-}$ mice. Sections in WT (A, E, I, M) or TS2$^{-/-}$/TS14$^{-/-}$ dorsal skin at distance (B, F, J, N), near (C, G, K, O) or at the border of lesions (D, H, L, P) were stained using antibodies specific to keratin 10 (A–D), Ki67 (E–H), CD45 (I–L) and with toluidine blue (M–P). The severity of the alterations increased at the immediate proximity of the lesions.*

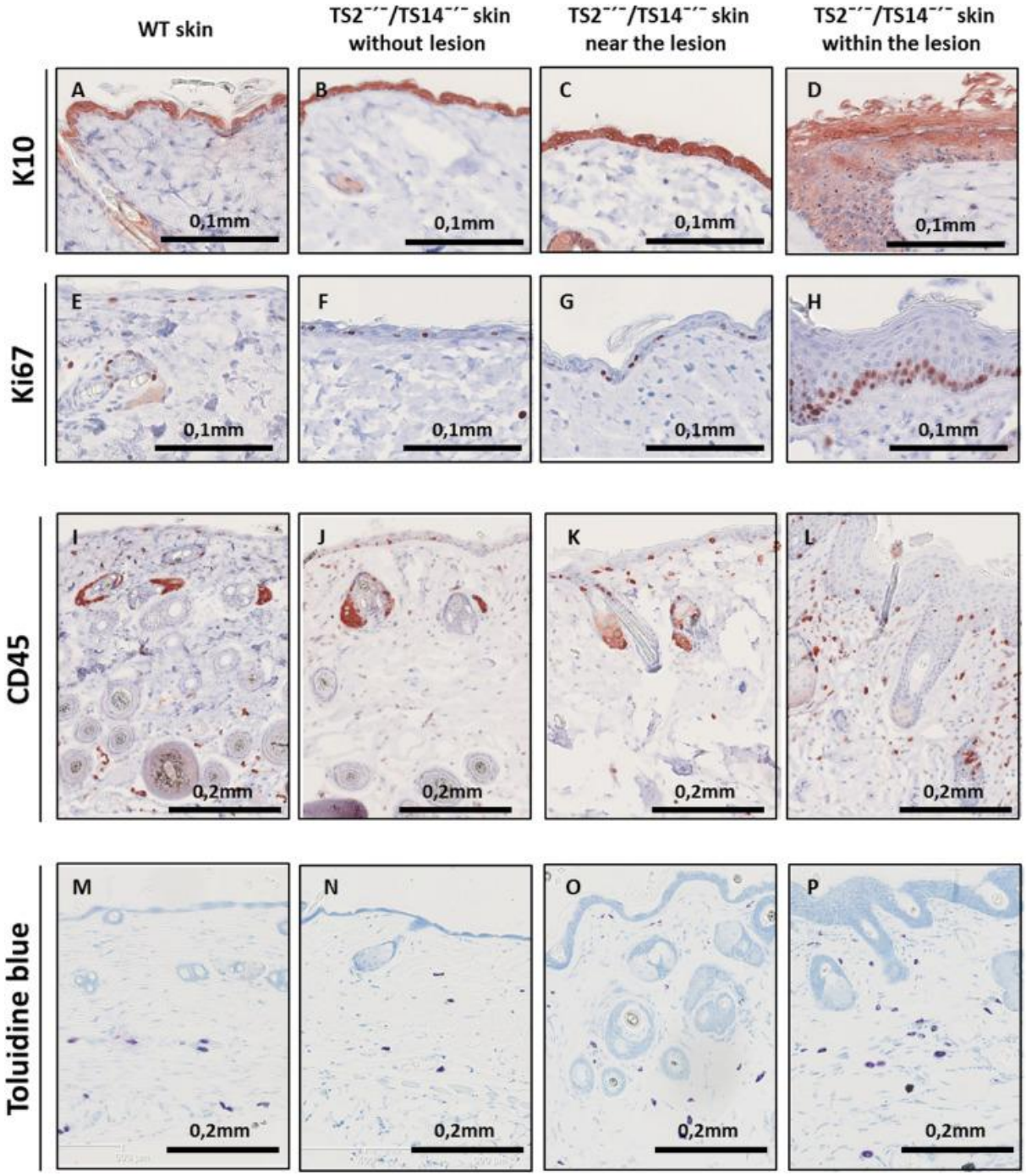

Published in : Matrix Biology (2018), vol. 70, pp. 140–157
DOI: https://doi.org/10.1016/j.matbio.2018.04.002
Status : Postprint (Author's version)

THE FORMATION OF CUTANEOUS LESIONS IN TS2$^{-/-}$/TS14$^{-/-}$ MICE IS NOT RELATED TO A GENERAL ALTERATION OF THE EPIDERMAL BARRIER AND IS NOT STIMULATED BY INDUCTION OF LOCAL INFLAMMATION

Spontaneous epidermal lesions can result from different primary causes such as alteration of the epidermal barrier. Histological analyses showed that the thick epidermis close to the lesions in TS2$^{-/-}$/TS14$^{-/-}$ mice was covered by an abundant stratum corneum and comprised a well-organized stratum granulosum, suggesting that the epithelial barrier was not significantly altered (Figure 7A).

To functionally characterize the barrier properties in the different mice, we measured the trans-epidermal water loss (TEWL). No difference was observed between the four genotypes (Figure 7B), indicating that the barrier function of the epidermis is not altered in TS2$^{-/-}$/TS14$^{-/-}$ mice.

ADAMTS2 and ADAMTS14 are reported to be expressed mainly in cells of mesenchymal origin, but also in subpopulations of macrophages (23). Immu-nofluorescence and immunohistochemical analyses of skin sections were performed in order to evaluate which cells are the highest producers and therefore have the highest likelihood to be implicated in the mechanisms leading to skin lesions in TS2$^{-/-}$/TS14$^{-/-}$ mice. None of the commercially available antibodies was sufficiently specific and effective to detect Adamts2 or Adamts14 on skin sections. Therefore, "*In Situ* Hybridization" was used as an alternative assay. The specificity of the hybridizations is illustrated in section of newborns, with positive staining in the spine and in the dermis (Figure S5 for *Adamts2*, Figure S6 for *Adamts14*). In adult healthy skin, however, only a weak non-specific staining was observed at the level of hair follicles. This suggests that the expression of *Adamts2* and *Adamts14* is too low in resting non activated fibroblasts to be detected by *in situ* hybridization and that cells with high expression of Adamts2 or 14 are absent or not common in healthy adult skin.

Although the skin phenotype inTS2$^{-/-}$/TS14$^{-/-}$ mice was not fully suggestive of an "epidermolysis bullosa" condition (for review [28]), we still decided to evaluate, by transmission electron microscopy, the integrity of the basement membrane separating the epidermis from the dermis. No difference in terms of structure and thickness could be evidenced between the different genotypes (Figure S7). Furthermore, the number and structure of the hemidesmosomes anchoring the basal layer of keratinocytes onto the basement membrane were also normal.

Different models were used to further evaluate the epidermal barrier function. Excessive skin dryness was induced in control and TS2$^{-/-}$/TS14$^{-/-}$ mice (8 week-old) by chronic application of an acetone/ ether (1:1) solution. A similar skin dryness was noted in all the mice, but the formation of epidermal lesions was never induced, explaining why this model was not investigated further.

As a complementary model to induce epidermal alterations, 8 week-old mice without lesion were topically treated with Imiquimod, an agonist of TLR7 inducing acute inflammation leading to psoriasis-like lesions. Redness and first signs of inflammation were observed in the 4 genotypes as soon as 24 h after the first application. After three additional applications, treated skins displayed psoriatic-like plaques, but similarly in the four genotypes. As expected, histological examinations clearly showed that Imiquimod induced the formation of a thick epidermis producing an abundant stratum corneum (Figure 8). Moderate leukocyte infiltration was also observed, but epidermal

Published in : Matrix Biology (2018), vol. 70, pp. 140–157
DOI: https://doi.org/10.1016/j.matbio.2018.04.002
Status : Postprint (Author's version)

lesions similar to those spontaneously appearing in older TS2$^{-/-}$/TS14$^{-/-}$ mice were never observed in any genotype.

***Figure 7**. Effectiveness of the skin barrier in TS2$^{-/-}$/TS14$^{-/-}$ mice. (A) Transversal sections were made in the skin ofTS2$^{-/-}$/TS14$^{-/-}$ mice at proximity of cutaneous lesions and stained with HE. The epidermis is covered by an abundant stratum corneum (arrow) and contains a well-organized stratum granulosum (arrowhead) suggesting that the quality of the epithelial barrier is not significantly altered. (B) The "trans-epidermal water loss" was measured (Tewameter, Courage + Khazaka) in order to have a functional evaluation of the epidermal barrier. 6 week-old mice of each genotype (n = 6) were used and none of them had visible skin lesion which could have skewed the measurements. Data are expressed in gram per square meter per hour (mean ± SD). Similar values were obtained for the four genotypes confirming that the quality of the skin barrier is normal in TS2$^{-/-}$/TS14$^{-/-}$ mice free of cutaneous lesions.*

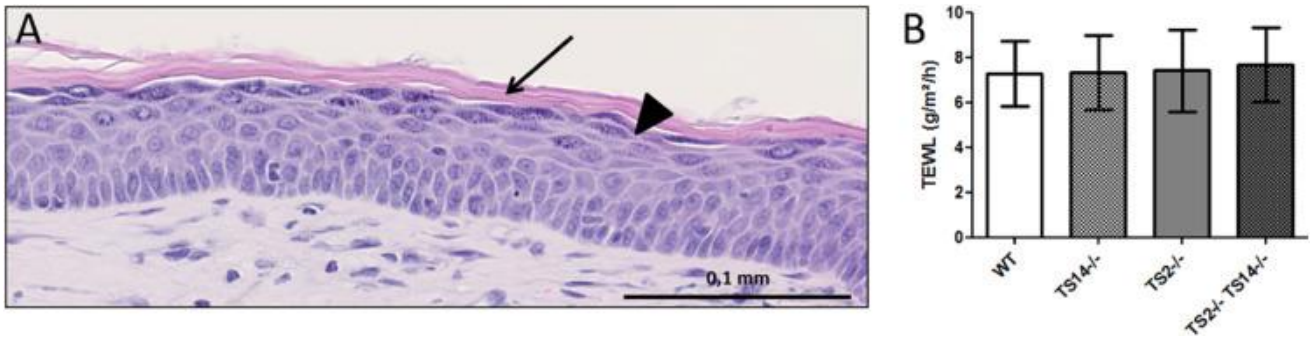

Published in : Matrix Biology (2018), vol. 70, pp. 140–157
DOI: https://doi.org/10.1016/j.matbio.2018.04.002
Status : Postprint (Author's version)

***Figure 8**. Induction of psoriasis-like alterations using Imiquimod. WT, TS2$^{-/-}$, TS14$^{-/-}$ and TS2$^{-/-}$/TS14$^{-/-}$ mice (n = 2 for each genotype) were treated by topical applications of Imiquimod (one daily application during 5 consecutive days). All mice developed psoriatic-like lesions with no difference between the 4 genotypes. Representative transversal sections of skin from WT (A) and TS2$^{-/-}$/TS14$^{-/-}$ mice (B) stained with HE are shown. Epidermis was thickened and cellularity was increased in the dermis due to inflammatory infiltrate and a higher fibroblastic density. No difference was observed between the genotypes and lesions similar to those appearing spontaneously in aging TS2$^{-/-}$/TS14$^{-/-}$ mice were never noticed.*

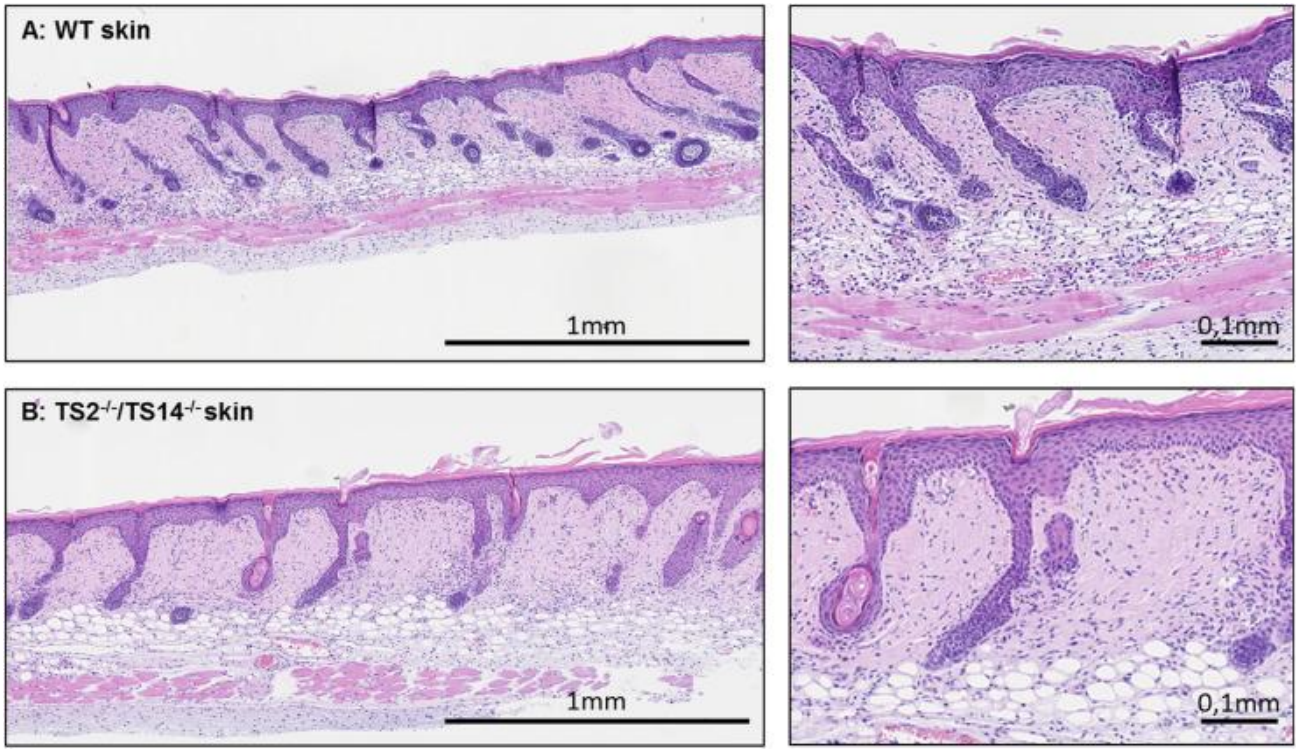

IMMUNOLOGICAL STATUS OF TS2$^{-/-}$/TS14$^{-/-}$ IS ALTERED BEFORE THE OCCURRENCE OF SKIN LESIONS

Other potential causes of atopic dermatitis-like skin lesions are related to dysregulation affecting the immune system. Skin sections from male TS2-/-/TS14-/- mice were systematically analyzed before the occurrence of lesions (≤8 weeks) and in unaffected skin of older mice at distant sites of the primary lesions to detect any potential specific distribution of immune cells. Some clusters of CD45 positive cells were observed in the apparently asymptomatic dermis (Figure 9A). Small clusters were also observed close to the epidermis where they seemed to trigger death of keratinocytes and local alterations of the epidermal barrier (Figure 9B, C and D).

Similar areas were then more specifically characterized on serial sections (Figure 10). A highly significant accumulation of T lymphocytes was observed within, and close to, the epidermis (Figure 10D, E). Increased level of IFNγ was noticed (Figure 10F) together with positive staining for cleaved

Published in : Matrix Biology (2018), vol. 70, pp. 140–157
DOI: https://doi.org/10.1016/j.matbio.2018.04.002
Status : Postprint (Author's version)

caspase 3 above the background level (Figure 10C). These immune cells are most probably causative of the local induction of apoptosis of keratinocytes, which secondarily leads to the localized disruption of the epidermal barrier and the onset of macroscopic epidermal lesions.

IMMUNE CELLS PROFILING IN BLOOD FROM WT AND TS2$^{-/-}$/ TS14$^{-/-}$ AT INCREASING AGE

Blood samples were collected in asymptomatic 8 week-old mice, and then 2 and 4 weeks later at times corresponding to increasing likelihood of developing lesions. FACS analyses showed that the total number of immune cells (Figure S8A, CD45^{+}) and the relative proportion of T lymphocytes (Figure S8D, CD3^{+}), granulocytes (Figure S8E, CD11b^{+}CD49b^{-}Gr1^{+}) and monocytes (Figure S8F, CD11b^{+}CD49b^{-}Gr1^{-}) were quite similar at the 3 time points for WT and TS2$^{-/-}$/TS14$^{-/-}$ mice, while moderate decreases in the number (Figure S8B) and relative proportions of B lymphocytes were noticed (Figure S8C, B220^{+}).

Among T lymphocytes, the proportion of CD4^{+} and CD8^{+} cells was slightly modified in opposite way (Figure 11A–B) but, most interestingly, they systemat-ically tended to be more activated (Figure 11C–D, ICOS^{+}) while their proliferation (Figure 11E–F, Ki67^{+}) was not reproducibly modified at the three time points (except for the CD4^{+} T cells in 8 week-old TS2$^{-/-}$/TS14$^{-/-}$ mice). The proportion and the functional activity of regulatory T cells (Tregs) were not modified (Figure S9).

***Figure 9**. Infiltration of immune cells in the asymptomatic skin of TS2$^{-/-}$/TS14$^{-/-}$ mice. Transversal sections of nonaffected skin from TS2$^{-/-}$/TS14$^{-/-}$ mice were stained using CD45 antibody. Accumulation of CD45 positive cells were observed locally in the dermal regions where skin lesions are still absent (A). Small clusters of immune cells were also sometimes localized in close contact with the epidermis where they appeared to progressively induce death of keratinocytes and rupture of the epidermis (B–D).*

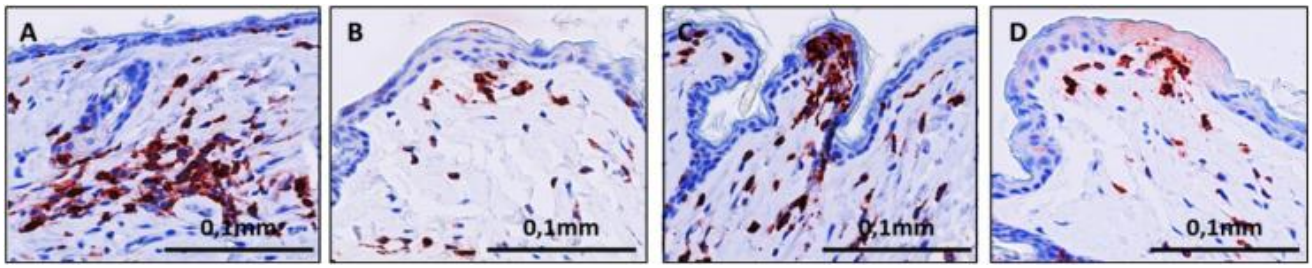

Published in : Matrix Biology (2018), vol. 70, pp. 140–157
DOI: https://doi.org/10.1016/j.matbio.2018.04.002
Status : Postprint (Author's version)

***Figure 10**. Characterization of the onset of epidermal lesion. Serial transverse sections in the skin of a young TS2$^{-/-}$/TS14$^{-/-}$ mouse without visible macroscopic lesion were stained using antibodies specific for CD45 (A, B), cleaved caspase 3 (C), CD3 (D, E) or IFN⊠ (F). Band Dare higher magnification pictures of the areas delineated bya rectangle in A and D, respectively. Pictures C and F were taken in the same location. CD45-positive leukocytes were scattered throughout the skin but could be sometimes observed as clusters close to the epidermis (A, B). Although T lymphocytes are rare in the skin (D), they constitute a large proportion of the immune cells forming the clusters (E). Apoptosis in the epidermis (C) and expression of IFNγ (F) were more specifically associated with immune cells accumulation.*

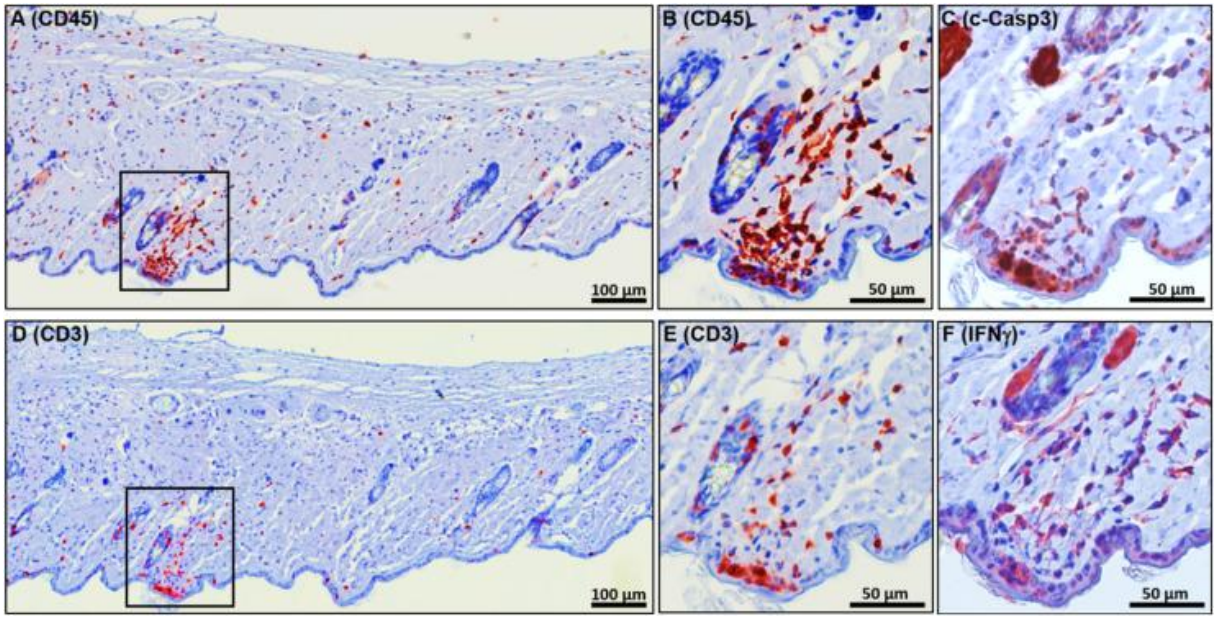

Published in : Matrix Biology (2018), vol. 70, pp. 140–157
DOI: https://doi.org/10.1016/j.matbio.2018.04.002
Status : Postprint (Author's version)

***Figure 11**. CD4⁺ and CD8⁺ T cell proportion and activation, but not proliferation, were modified in blood of TS2⁻/⁻/TS14⁻/⁻ mice. As compared to WT, the proportions of CD4⁺ (A) and CD8⁺ (B) among T cells were modified in TS2⁻/⁻/TS14⁻/⁻ mice. The percentages of activated cells (ICOS⁺) also tended to be higher at the 3 time-points (C, D) while proliferation was not reproducibly altered (E, F). *P < 0.05; **P < 0.01.*

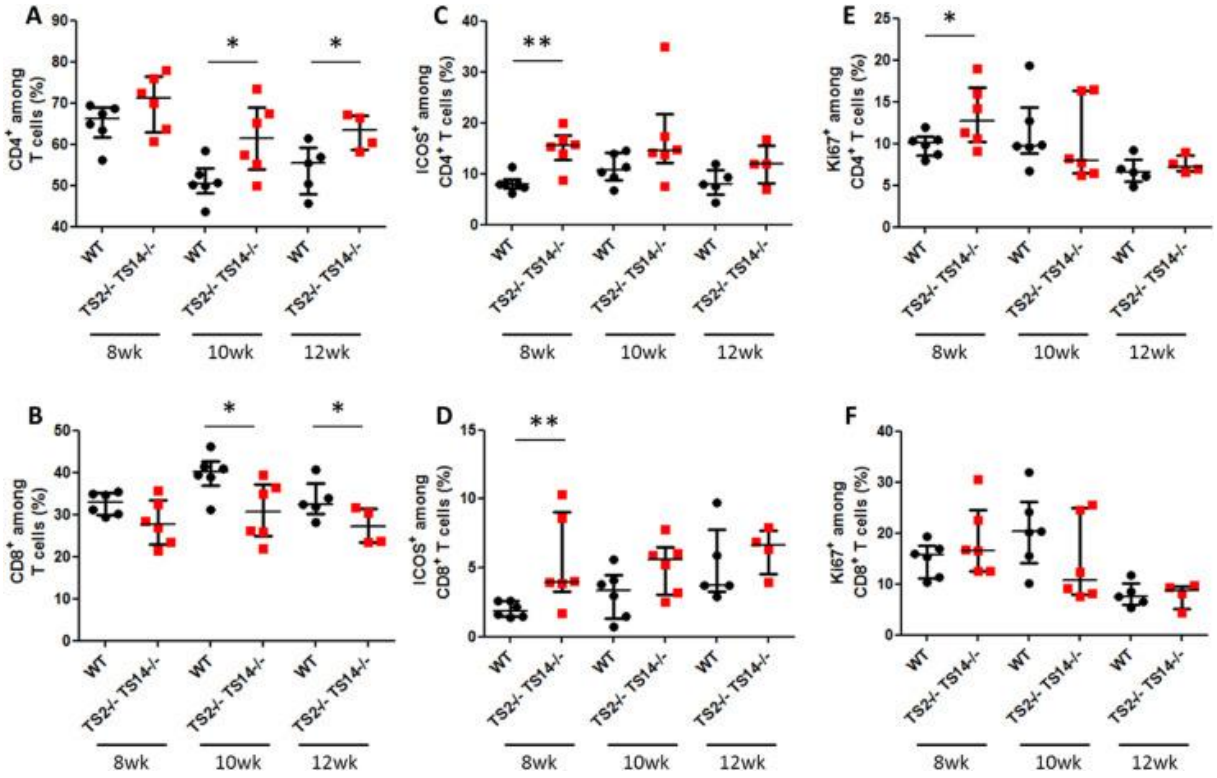

IMMUNOLOGICAL STATUS OF THE FOUR GENOTYPES AT 8 WEEKS

To evaluate the potential influence of the deletion of Adamts2 or Adamts14 alone, analyses of the immunological status were also performed on 8 week-old WT, TS2⁻/⁻, TS14⁻/⁻ and TS2⁻/⁻/TS14⁻/⁻ mice. In blood, the number and general profile of immune cells were similar for the 4 groups, except for an increase of the proportion of T lymphocytes, especially of the CD4⁺ T-helper cell lineage (Figure S10). Increased activation (Figure 12A, ICOS⁺) and proliferation (Figure 12B, Ki67⁺) of CD4⁺ T cells were observed only in TS2⁻/⁻/TS14⁻/⁻ mice. The respective proportions of CD4⁺ cells being also CD44⁺ (effector memory CD4⁺ cells) or CD62L⁺ (naïve CD4⁺ cells) were also significantly altered (Figure 12C–D). Similar analyses were performed on cells recovered from the spleen. As in blood, CD4⁺ T cells from TS2⁻/⁻/TS14⁻/⁻ mice were more activated (ICOS⁺, E) and more proliferative (KI67, F), and displayed alterations of their differen-tiation status (G, H) as compared to WT cells. Clear trends of modifications of proliferation and differentiation were also identified forCD4⁺ T cells from TS2⁻/⁻ and TS14⁻/⁻ mice (F, H). These data were further confirmed through experiments quantifying the % of CD4⁺ T cells expressing IL-2 (Figure 12I) and IFNγ (Figure 12J), two Th1 cytokines.

Published in : Matrix Biology (2018), vol. 70, pp. 140–157
DOI: https://doi.org/10.1016/j.matbio.2018.04.002
Status : Postprint (Author's version)

***Figure 12**. CD4⁺ T cells activation and proliferation in blood and in spleen from WT, TS14⁻/⁻, TS2-/- and TS2⁻/⁻/TS14⁻/⁻. FACS analyses were performed on blood and spleen of 8 week-old mice. In blood (A-D), increased activation (ICOS⁺, A) and proliferation (Ki67⁺, B) of CD4⁺ T cells was observed only in TS2⁻/⁻/TS14⁻/⁻ mice. Increase of effector memory (CD44⁺, C) and decrease of naive (CD62L⁺, D) CD4⁺ T cells frequency in blood from TS2⁻/⁻/TS14⁻/⁻ mice were also observed. In the spleen (E–J), an increased activation (ICOS⁺, E) of CD4⁺ T cells was observed in TS2⁻/⁻/TS14⁻/⁻ mice only. Higher proliferation (Ki67⁺, F) was observed for TS14⁻/⁻, TS2⁻/⁻ and TS2⁻/⁻/TS14⁻/⁻ mice, as well as trends towards an increase of effector memory (CD44⁺, G) and a decrease of naive (CD62L⁺, H) CD4⁺ T cells frequency. The proportion of CD4⁺ cells expressing IL-2 (I) or IFNγ (J), two Th1 cytokines, was increased in TS2⁻/⁻/TS14⁻/⁻ mice but also in TS14⁻/⁻ mice. *P < 0.05; **P < 0.01; ***P < 0.001.*

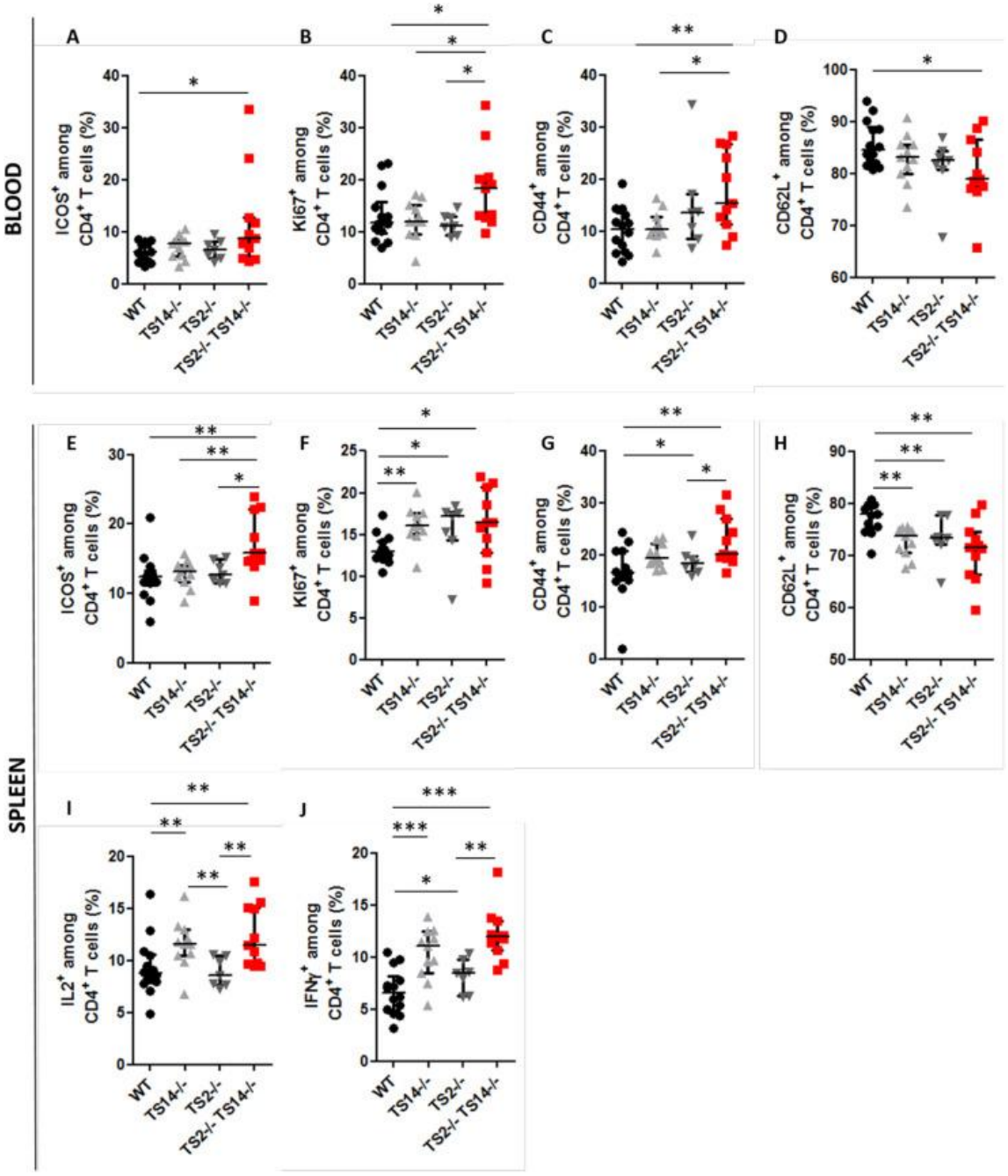

Published in : Matrix Biology (2018), vol. 70, pp. 140–157
DOI: https://doi.org/10.1016/j.matbio.2018.04.002
Status : Postprint (Author's version)

NON IMMUNE EVENTS ARE THE CAUSES OF THE IMMUNE ACTIVATION LEADING TO EPIDERMAL LESIONS IN TS2$^{-/-}$/TS14$^{-/-}$ MICE

In order to evaluate if the immune dysregulations are related to alteration of the immune system itself or to its environment, bone marrow cells from WT mice were grafted in irradiated TS2$^{-/-}$/TS14$^{-/-}$ mice, and vice versa. It has to be noted that 8 week-old male mice were used and that TS2$^{-/-}$/TS14$^{-/-}$ mice did not display any visible epidermal lesions at the beginning of the experiment. Six TS2$^{-/-}$/TS14$^{-/-}$ mice were irradiated, from which 5 were grafted with WT bone marrow and one with TS2$^{-/-}$/TS14$^{-/-}$ bone marrow, as control. An identical experimental design was used for the six irradiated WT mice (5 grafted with TS2$^{-/-}$/TS14$^{-/-}$ bone marrow and 1 with WT bone marrow). After 3 months, the 6 irradiated WT mice had survived and did not display any sign of cutaneous lesion. The TS2$^{-/-}$/TS14$^{-/-}$ mouse grafted with TS2$^{-/-}$/TS14$^{-/-}$ bone marrow cells developed lesions, as expected. Regarding the TS2$^{-/-}$/TS14$^{-/-}$ irradiated mice receiving WT bone marrow, 2 died from infection and intestinal problems while the 3 remaining mice developed lesions 4, 7 (Figure 13) or 11 weeks after the transplant, which corresponded to the expected onset of the phenotype.

Figure 13. *Hematoxylin-eosin staining of skin with lesions from TS2$^{-/-}$/TS14$^{-/-}$ mice grafted with WT bone marrow. Transversal sections of skin with lesions from TS2$^{-/-}$/TS14$^{-/-}$ mice grafted with WT bone marrow were stained with HE. At the lesion site, both epidermal rupture and keratinocytes hyperproliferation can be seen. Infiltration of immune cells in the dermis and a high number of blood vessels are observed in the lesional zone.*

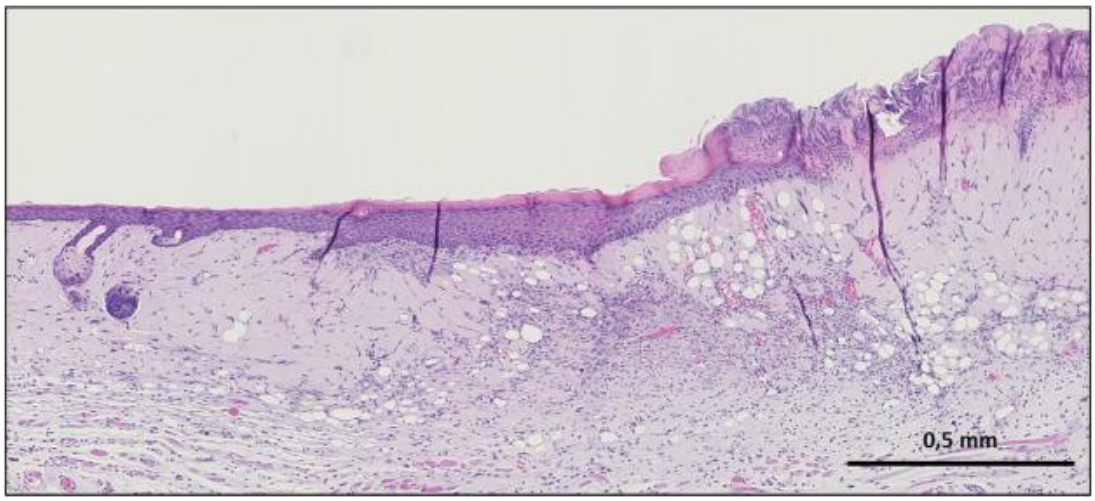

Published in : Matrix Biology (2018), vol. 70, pp. 140–157
DOI: https://doi.org/10.1016/j.matbio.2018.04.002
Status : Postprint (Author's version)

Discussion

ADAMTS2, 3 and 14 are highly similar enzymes in terms of sequence and domain organization [29]. Among the ADAMTS family, they form the "amino-procollagen peptidase" sub-family, a name describing the first identified function of ADAMTS2: the excision of the aminopropeptide of fibrillar procollagens [6,14]. Recently, ADAMTS3, but not ADAMTS2 or ADAMTS14, was found to be crucial for the proteolytic activation of pro-VEGF-C into active VEGF-C able to drive embryonic lymphangiogenesis [17,18]. The knowledge and data regarding ADAMTS14 are much scarce and often indirect. For instance, genetic linkage analyses have identified ADAMTS14 as a gene potentially involved in multiple sclerosis [20] and osteoarthritis [21].

Here we have generated *Adamts14*$^{-/-}$ (TS14$^{-/-}$) mice to gain a better insight into the biological functions of ADAMTS14. These mice are healthy, fertile and display no obvious phenotype. The maturation of type I and type III fibrillar collagens in the main connective tissues, such as skin, tendon or bone, is also normal, suggesting that ADAMTS14 is not a major aminoprocollagen peptidase *in vivo*. However, it does not rule out the possibility that ADAMTS14 could act as an ancillary enzyme, especially when ADAMTS2 is defective. Indeed, it has been described that the processing of the aminopropeptide of type I procolla-gen is far from being completely prevented in absence of active ADAMTS2 [14]. In *Adamts2*$^{-/-}$ mice (TS2$^{-/-}$), as in human patients with the dermatosparactic type of Ehlers-Danlos syndrome, the percentage of fully matured type I collagen varies from 20 to 30% in the skin to 80% in tendons and almost 100% in bone, which indicates the existence of another enzyme able to compensate for the absence of ADAMTS2 activity. In order to evaluate if ADAMTS14 could be responsible for this compensatory activity, we generated mice deficient for both *Adamts2* and *Adamts14* (TS2$^{-/-}$/TS14$^{-/-}$). These doubly deficient mice are viable and displayed initially the same phenotype as TS2$^{-/-}$ mice [13], with a ruffled aspect of their fur, male sterility and severe skin fragility caused by the accumulation of abnormal collagen fibrils in the dermis. Mechanical properties of the skin of the different genotypes were also determined. Elongation and tensile strength at rupture are similar in wild type and TS14$^{-/-}$ mice, while they are strongly and similarly altered in both TS2$^{-/-}$ and TS2$^{-/-}$/TS14$^{-/-}$ mice. Altogether the data indicate that ADAMTS14 is not involved in procollagen processing *in vivo*, even as a minor and ancillary enzyme, and that other enzymes, potentially meprins [30], can supplement the absence of ADAMTS2 activity.

Unexpectedly, formation of superficial scabs was observed in TS2$^{-/-}$/TS14$^{-/-}$ mice, occurring mainly in males at a mean age of 13 weeks. Similar lesions were never found neither in TS14$^{-/-}$ mice nor in TS2$^{-/-}$ mice, which indicates that the structural alteration of collagen fibrils and dermal fragility are not involved in this peculiar phenotype. Histological evaluations clearly confirmed that the lesions are always superficial and do not result from dermal damage. Hypertrophic epidermis and hyper-cellularity in the dermis were striking close to the lesions but never observed a few millimeters away where skin seems to remain healthy, suggesting that these features are the consequence and not the primary cause of the epidermal lesions.

In human, epidermal alterations are found in several inherited or acquired pathologies, such as epidermolysis bullosa (EB), psoriasis, systemic lupus erythematosus (SLE) and atopic dermatitis

Published in : Matrix Biology (2018), vol. 70, pp. 140–157
DOI: https://doi.org/10.1016/j.matbio.2018.04.002
Status : Postprint (Author's version)

(AD). EB is characterized by blistering and erosion of the epidermis and caused by mutations in proteins involved in the formation of the cutaneous basement membrane or in the anchoring of keratinocytes to the basement membrane [28]. However, blisters were never observed in TS2$^{-/-}$/TS14$^{-/-}$ mice and the basement membrane was shown to be normal by electron microscopy. In psoriasis, the epidermis is hypertrophic and characterized by the presence of an abundant stratum corneum [31], but focal epidermal rupture as seen in TS2$^{-/-}$/TS14$^{-/-}$ skin are not common. Furthermore, stimulation of TLR7 by Imiquimod, a recognized model of induced psoriatic-like skin [32,33], gave similar alterations in the four genotypes, but did not induce the formation of epidermal lesions similar to those appearing spontaneously in TS2$^{-/-}$/ TS14$^{-/-}$ mice, indicating that the involved pathological mechanisms should be different.

In TS2$^{-/-}$/TS14$^{-/-}$ mice, the integrity and the efficacy of the epidermal barrier does not seem to be significantly altered, as judged from histological examinations and trans-epidermal water loss (TEWL) measurements. Furthermore, induction of skin dryness and permeability by chemicals did not promote the formation of epidermal lesions, suggesting that dysfunction of the epidermal barrier is not the primary cause of the phenotype. The implication of the immune system was therefore evaluated. Asymptomatic young TS2$^{-/-}$/TS14$^{-/-}$ mice and their age-matched controls (WT, TS2$^{-/-}$ and TS14$^{-/-}$) were used to evaluate a potential immune dysregulation before the occurrence of cutaneous manifestations. FACS analyses indicate that the most consistent differences between TS2$^{-/-}$/ TS14$^{-/-}$ mice and their WT controls were related to T lymphocytes which were more activated and secreted higher levels of IL-2 and IFNγ. Similar trends were also observed for both cytokines in TS14$^{-/-}$ mice and for IFNγ in TS2$^{-/-}$ despite the fact that they never develop epidermal lesions. This observation suggests that the absence of these two enzymes has a direct global impact in the regulation of the immune system, and not only at the skin level. Immunohistochemical analyses of non-lesional skin of TS2$^{-/-}$/TS14$^{-/-}$ mice revealed the presence of immune cells clusters, mainly T lymphocytes, in the dermis or in contact with the epidermis where they seem to induce the apoptosis of keratinocytes and localized epidermal rupture. Altogether, these observations showed that dysregulation of the immune system in TS2$^{-/-}$/TS14$^{-/-}$ mice precedes and causes the epidermal lesions. However, the primary molecular defect is probably not directly related to the immune system itself since TS2$^{-/-}$/TS14$^{-/-}$ mice grafted with WT immune cells still developed lesions.

T lymphocytes are directly involved in the pathogeny of SLE [34] and AD [35]. SLE is a human immune disease affecting mostly females [36]. A reduction of IL- 2 synthesis is considered to be a driver of the disease by allowing a progressive Th17 polarization. A decreased TReg activity is also a key mechanism in the evolution of SLE [34]. In TS2$^{-/-}$/TS14$^{-/-}$ mice, TReg are not affected, the synthesis of IL-2 is increased and lesions occur mostly in males, suggesting that these mice do not represent a SLE-like syndrome. AD is a multifactorial and complex syndrome which is more common during childhood, but might affect equally males and females at any age [35]. It involves alterations of the epithelial barrier and activation of the immune system, two mechanisms strengthening each other and progressively leading to the worsening of the phenotype with epidermal eczematous lesions, immune infiltration and inflammation in other organs such as lung and intestine [37]. Although still controversial, AD can be divided in two distinct entities, referred as extrinsic and intrinsic [38]. Extrinsic AD results from immunization to foreign allergens and is characterized by elevated IgE,

Published in : Matrix Biology (2018), vol. 70, pp. 140–157
DOI: https://doi.org/10.1016/j.matbio.2018.04.002
Status : Postprint (Author's version)

eosinophilic infiltration and a Th2 response with a high production of IL-4. In most cases, its primary cause is a defect in the epidermal barrier allowing penetration and contacts with allergens. The intrinsic AD is less well defined but an abnormal activation of innate immunity and/or production of autoantibodies against components of the epidermis seem to be involved [38]. In human intrinsic AD the Th2 response is absent, there is no production of IgE and no eosinophilic infiltration, but rather a Th1/Th17/Th22 dominance with a high production of IFNγ [39], which is reminiscent of what is observed in our TS2$^{-/-}$/TS14$^{-/-}$ mice.

The reasons why double deficiency in Adamts2 and Adamts14 is required to induce epidermal lesions and the nature of molecular mechanisms leading to activation of the immune system are still open questions.

Several hypotheses can be made based on our current knowledge about the potential and validated substrates of ADAMTS2 and 14 [40], but also regarding cells which produce them *in vivo*. ADAMTS are secreted enzymes, meaning that they can cleave substrates that are at some distance of the producing cells. ADAMTS2 is mostly expressed by cells of mesenchymal origin (fibroblasts, adipocytes, smooth muscle cells, mesenchymal stem cells) and, to a much lower extent, in some other tissues or cells such as spleen and activated macrophages. Many cell types, such as keratinocytes, do not display any detectable level of expression. ADAMTS14 is similarly distributed as ADAMTS2 but with lower levels of expression. We have recently demonstrated that ADAMTS2 and ADAMTS14 can cleave several factors participating in the TGFβ pathway and that inhibition of ADAMTS2 in fibroblasts represses their response to TGFβ1 or TGFβ2 [40]. Since the TGFβ pathway and mesenchymal stem cells are both strongly involved in the regulation of several key pathways stimulating or repressing the immune system [41,42], the hypothesis of their direct implications in the phenotype of the TS2$^{-/-}$/TS14$^{-/-}$ mice would be worth to be evaluated in priority. Several factors of the innate immunity such as C1q, ficollins, collectins, adiponectin and mannose binding lectin (MBL) are other potential substrates of ADAMTS2 and ADAMTS14, since they contain a "collagen" domain shorter but similar to the triple helical domain found in fibrillar collagens [43], the first identified substrates of ADAMTS2 and 14. Other potential substrates are those containing TSR1 repeats such as properdin. Different elements hamper a straightforward identification of the substrates responsible for, or at least involved in, the peculiar phenotype in the TS2$^{-/-}$/TS14$^{-/-}$ mice. These candidate substrates might be expressed at low level or at high level but in a very low number of cells, such as some subtypes of resident or infiltrating immune cells present in the skin, which would prevent their identification from crude extracts and would require specifically dedicated enrichment procedures such as immunoprecipitation. Furthermore, the cleavage of a substrate close to its NH2- or the COOH-extremities can dramatically change its biological activities without changing significantly its size and its electrophoretic mobility, preventing the identification of such substrates by Western blot. Finally, although the main phenotype is seen in the skin, we cannot exclude that the primary alterations occur in a distant tissue involved in the regulation of the immune system, such as spleen, thymus or bone marrow. In order to overcome all these potential pitfalls, an integrated analysis, which will use different tissue samples, purified enzymes and the cutting-edge N-TAILS proteomic analysis [40], is currently being designed, but will go well beyond the objectives of this study.

Published in : Matrix Biology (2018), vol. 70, pp. 140–157
DOI: https://doi.org/10.1016/j.matbio.2018.04.002
Status : Postprint (Author's version)

Here we have demonstrated that ADAMTS2 and ADAMTS14 participate to the regulation of the activation of the immune system and that their simultaneous deficiency leads to an intrinsic atopic dermatitis-like syndrome. This study therefore highlights the existence of critical additional functions for these two enzymes initially described for their role in collagen maturation and matrix biology.

Authorship contributions

DL, EG, NB, BF and CA designed the research. DL and EG performed the research with help of CM, MC, LC, JL and DJ. CD participated to the analysis of (immuno)histological sections. TM performed electron microscopy pictures. JC and TJM were involved in the evaluation of the mechanical properties of the skin samples. DL and CA wrote the manuscript. All authors reviewed the results and approved the final version of the manuscript.

Acknowledgements

A special thanks to Antoine Heyeres and Lola Vanoorschot for excellent technical assistance. Alain Colige is a "Senior Research Associate" of the FRS-FNRS, and LD is supported by a "Télévie" grant (7459517F and 7453114F). The supports of the FRS-FNRS (FRSM, T.0183.13), the "Fonds Léon Frédéricq" (Grant to LD) and the "Centre anticancéreux" (Grant to LD) are also acknowledged. A thanks to Marie-Alix Sauvage, CK Technology, Visé for lending us the Tewameter. A thanks to GIGAMouse facility platform of University of Liège.

Appendix A. Supplementary data

Supplementary data to this article can be found online at :

https://doi.org/10.1016/j.matbio.2018.04.002.

Published in : Matrix Biology (2018), vol. 70, pp. 140–157
DOI: https://doi.org/10.1016/j.matbio.2018.04.002
Status : Postprint (Author's version)

References

[1] S.S. Apte, W.C. Parks, Metalloproteinases: a parade of functions in matrix biology and an outlook for the future, Matrix Biol. 44–46 (May–Jul 2015) 1–6.

[2] S.S. Apte, A disintegrin-like and metalloprotease (reprolysintype) with thrombospondin type 1motif (ADAMTS) superfamily: functions and mechanisms, J. Biol. Chem. 284 (2009) 31493–31497.

[3] J. Dubail, S.S. Apte, Insights on ADAMTS proteases and ADAMTS-like proteins from mammalian genetics, Matrix Biol. 44–46 (May–Jul 2015) 24–37.

[4] D.R. Hopkins, S. Keles, D.S. Greenspan, The bone morphogenetic protein 1/Tolloid-like metalloproteinases, Matrix Biol. 26 (7) (Sep 2007) 508–523.

[5] S. Vadon-Le Goff, D.J. Hulmes, C. Moali, BMP-1/tolloid-like proteinases synchronize matrix assembly with growth factor activation to promote morphogenesis and tissue remodeling, Matrix Biol. 44–46 (May–Jul 2015) 14–23.

[6] A. Colige, F. Ruggiero, I. Vandenberghe, J. Dubail, F. Kesteloot, J. Van Beeumen, A. Beschin, L. Brys, C.M. Lapiere, B. Nusgens, Domains and maturation processes that regulate the activity of ADAMTS-2, a metalloproteinase cleaving the aminopropeptide of fibrillar procollagens types I–III and V, J. Biol. Chem. 280 (2005) 34397–34408.

[7] A. Colige, A. Beschin, B. Samyn, Y. Goebels, J. Van Beeumen, B.V. Nusgens, C.M. Lapière, Characterization and partial amino acid sequencing of a 107-kDa procollagen I N-proteinase purified by affinity chromatography on immobilized type XIV collagen, J. Biol. Chem. 270 (28) (1995) 16724–16730.

[8] A. Colige, S.W. Li, A.L. Sieron, B.V. Nusgens, D.J. Prockop, C.M. Lapière, cDNA cloning and expression of bovine procollagen I N-proteinase: a new member of the superfamily of zinc-metalloproteinases with binding sites for cells and other matrix components, Proc. Natl. Acad. Sci. U. S. A. 94 (6) (1997) 2374–2379.

[9] D.J. Prockop, A.L. Sieron, S.W. Li, Procollagen N-proteinase and procollagen C-proteinase. Two unusual métalloprotéinases that are essential for procollagen processing probably have important roles in development and cell signaling, Matrix Biol. 16 (7) (1998) 399–408.

[10] R.J. Fernandes, S. Hirohata, J.M. Engle, A. Colige, D.H. Cohn, D.R. Eyre, S.S. Apte, Procollagen II amino propeptide processing by ADAMTS-3. Insights on dermatosparaxis, J. Biol. Chem. 276 (2001) 31502–31509.

[11] A. Colige, A.L. Sieron, S.W. Li, U. Schwarze, E. Petty, W. Wertelecki, W. Wilcox, D. Krakow, D.H. Cohn, W. Reardon, et al., Human Ehlers-Danlos syndrome type VII C and bovine dermatosparaxis are caused by mutations in the procollagen I N-proteinase gene, Am. J. Hum. Genet. 65 (1999) 308–317.

[12] A. Colige, L. Nuytinck, I. Hausser, A.J. van Essen, M. Thiry, C. Herens, L.C. Ades, F. Malfait, A.D. Paepe, P. Franck, et al., Novel types of mutation responsible for the dermatosparactic type of Ehlers-Danlos syndrome (Type VIIC) and common polymorphisms in the ADAMTS2 gene, J. Invest. Dermatol. 123 (2004) 656–663.

[13] S.W. Li, M. Arita, A. Fertala, Y. Bao, G.C. Kopen, T.K. Langsjo, M.M. Hyttinen, H.J. Helminen, D.J. Prockop,Transgenic mice with inactive alleles for procollagen Nproteinase (ADAMTS-2) develop fragile skin and male sterility, Biochem. J. 355 (2001) 271–278.

[14] A. Colige, I. Vandenberghe, M. Thiry, C.A. Lambert, J. Van Beeumen, S.W. Li, D.J. Prockop, C.M. Lapiere, B.V. Nusgens, Cloning and characterization of ADAMTS-14, a novel ADAMTS displaying high homology with ADAMTS-2 and ADAMTS-3, J. Biol. Chem. 277 (2002) 5756–5766.

Published in : Matrix Biology (2018), vol. 70, pp. 140–157
DOI: https://doi.org/10.1016/j.matbio.2018.04.002
Status : Postprint (Author's version)

[15] C. Le Goff, R.P. Somerville, F. Kesteloot, K. Powell, D.E. Birk, A.C. Colige, S.S. Apte, Regulation of procollagen aminopropeptide processing during mouse embryogenesis by specialization of homologous ADAMTS proteases: insights on collagen biosynthesis and dermatosparaxis, Development 133 (2006) 1587–1596.

[16] F. Kesteloot, A. Desmoulière, I. Leclercq, M. Thiry, J.E. Arrese, D.J. Prockop, C.M. Lapière, B.V. Nusgens, A. Colige, ADAM metallopeptidase with thrombospondin type 1 motif 2

inactivation reduces the extent and stability of carbon tetrachloride-induced hepatic fibrosis in mice, Hepatology 46 (2007) 1620–1631.

[17] L. Janssen, L. Dupont, M. Bekhouche, A. Noel, C. Leduc, M. Voz, B. Peers, D. Cataldo, S.S. Apte, J. Dubail, A. Colige, ADAMTS3 activity is mandatory for embryonic lymphangiogenesis and regulates placental angiogenesis, Angiogenesis 19 (2015) 53–65.

[18] M. Jeltsch, S.K. Jha, D. Tvorogov, A. Anisimov, V.M. Leppänen, T. Holopainen, R. Kivelä, S. Ortega, T. Kärpanen, K. Alitalo, CCBE1 enhances lymphangiogenesis via ADAMTS3-mediated VEGF-C activation, Circulation 129 (2014) 1962–1971.

[19] P. Brouillard, L. Dupont, R. Helaers, R. Coulie, G.E. Tiller, J. Peeden, A. Colige, M. Vikkula, Loss of ADAMTS3 activity causes Hennekam lymphangiectasia-lymphedema syndrome 3, Hum. Mol. Genet. (21) (2017) 4095–4104.

[20] R. Goertsches, M. Comabella, A. Navarro, H. Perkal, X. Montalban, Genetic association between polymorphisms in the ADAMTS14 gene and multiple sclerosis, J. Neuroimmunol. 164 (2005) 140–147.

[21] J. Rodriguez-Lopez, M. Pombo-Suarez, J. Loughlin, A. Tsezou, F.J. Blanco, I. Meulenbelt, P.E. Slagboom, A.M. Valdes, T.D. Spector, J.J. Gomez-Reino, A. Gonzalez, Association of a nsSNP in ADAMTS14 to some osteoarthritis phenotypes, Osteoarthr. Cartil. 17 (2009) 321–327.

[22] J. Dubail, F. Kesteloot, C. Deroanne, P. Motte, V. Lambert, J. M. Rakic, C. Lapiere, B. Nusgens, A. Colige, ADAMTS-2 functions as anti-angiogenic and anti-tumoral molecule independently of its catalytic activity, Cell. Mol. Life Sci. 67 (2010) 4213–4232.

[23] T.P. Hofer, M. Frankenberger, J. Mages, R. Lang, P. Meyer, R. Hoffmann, A. Colige, L. Ziegler-Heitbrock, Tissue-specific induction of ADAMTS2 in monocytes and macrophages by glucocorticoids, J. Mol. Med. 86 (2008) 323–332.

[24] A. Arning, M. Hiersche, A. Witten, G. Kurlemann, K. Kurnik, D. Manner, M. Stoll, U. Nowak-Gottl, A genome-wide association study identifies a gene network of ADAMTS genes in the predisposition to pediatric stroke, Blood 120 (2012) 5231–5236.

[25] C.W. Lee, I. Hwang, C.S. Park, H. Lee, D.W. Park, S.J. Kang, S.W. Lee, Y.H. Kim, S.W. Park, S.J. Park, Expression of ADAMTS-2, -3, -13, and -14 in culprit coronary lesions in patients with acute myocardial infarction or stable angina, J. Thromb. Thrombolysis 33 (2012) 362–370.

[26] T. Shigeoka, M. Kawaichi, Y. Ishida, Suppression of nonsense-mediated mRNA decay permits unbiased genetrapping in mouse embryonic stem cells, Nucleic Acids Res. 33 (2005), e20.

[27] C. Le Goff, F. Morice-Picard, N. Dagoneau, L.W. Wang, C. Perrot, Y.J. Crow, F. Bauer, E. Flori, C. Prost-Squarcioni, D. Krakow, G. Ge, D.S. Greenspan, D. Bonnet, M. Le Merrer, A. Munnich, S.S. Apte, V. Cormier-Daire, ADAMTSL2 mutations in geleophysic dysplasia demonstrate a role for ADAMTSlike proteins in TGF-beta bioavailability regulation, Nat. Genet. 40 (2008) 1119–1123.

Published in : Matrix Biology (2018), vol. 70, pp. 140–157
DOI: https://doi.org/10.1016/j.matbio.2018.04.002
Status : Postprint (Author's version)

[28] J. Uitto, C. Has, H. Vahidnezhad, L. Youssefian, L. Bruckner-Tuderman, Molecular pathology of the basement membrane zone in heritable blistering diseases: the paradigm of epidermolysis bullosa, Matrix Biol. 57–58 (2017) 76–85.

[29] M. Bekhouche, A. Colige, The procollagen N-proteinases ADAMTS2, 3 and 14 in pathophysiology, Matrix Biol. 44–46 (2015) 46–53.

[30] J. Prox, P. Arnold, C. Becker-Pauly, Meprin α and meprin β: procollagen proteinases in health and disease, Matrix Biol. 44–46 (May–Jul 2015) 7–13.

[31] P. Di Meglio, F. Villanova, F.O. Nestle, Psoriasis, CSH Perspect. Med. 8 (2014) 1–4.

[32] L. van der Fits, S. Mourits, J.S. Voerman, M. Kant, L. Boon, J. D. Laman, F. Cornelissen, A.M. Mus, E. Florencia, E.P. Prens, E. Lubberts, Imiquimod-induced psoriasis-like skin inflammation in mice is mediated via the IL-23/IL-17 axis, J. Immunol. 182 (2009) 5836–5845.

[33] Y. Cai, X. Shen, C. Ding, C. Qi, K. Li, X. Li, V.R. Jala, H.G. Zhang, T. Wang, J. Zheng, J. Yan, Pivotal role of dermal IL-17-producing gammadelta T cells in skin inflammation,

Immunity 35 (2011) 596–610.

[34] A. Kaul,C.Gordon, M.K. Crow, Z. Touma,M.B.Urowitz, R. van Vollenhoven, G. Ruiz-Irastorza, G. Hughes, Systemic lupus erythematosus, Nat. Rev. Dis. Primers 2 (2016) (n° 16039).

[35] J. Levin, S. Fallon Friedlander, J.Q.Del Rosso, Atopic dermatitis and the stratum corneum: part 3: the immune system in atopic dermatitis, J. Clin. Aesthet. Dermatol. 6 (2013) 37–44.

[36] E.C. Somers, W. Marder, P. Cagnoli, E.E. Lewis, P. DeGuire, C. Gordon, C.G. Helmick, L. Wang, J.J. Wing, J.P. Dhar, J. Leisen, D. Shaltis, W.J. McCune, Population-based incidence and prevalence of systemic lupus erythematosus: the Michigan lupus epidemiology and surveillance program, Arthritis Rheumatol. 66 (2014) 369–378.

[37] T. Bieber, Atopic dermatitis, N. Engl. J. Med. 358 (2008) 1483–1494.

[38] Y. Tokura, Extrinsic and intrinsic types of atopic dermatitis, J. Dermatol. Sci. 58 (2010) 1–7.

[39] K. Eyerich, N. Novak, Immunology of atopic eczema: overcoming the Th1/Th2 paradigm, Allergy 68 (2013) 974–982.

[40] M. Bekhouche, C. Leduc, L. Dupont, L. Janssen, F. Delolme, S. Vadon-Le Goff, N. Smargiasso, D. Baiwir, G. Mazzucchelli, I. Zanella-Cleon, J. Dubail, E. De Pauw, B. Nusgens, D.J. Hulmes, C. Moali, A. Colige, Determination of the substrate repertoire of ADAMTS2, 3, and 14 significantly broadens their functions and identifies extracellular matrix organization and TGF-β signaling as primary targets, FASEB J. 30 (2016) 1741–1756.

[41] N. Li, J.Hua, Interactions between mesenchymal stem cells and the immune system, Cell. Mol. Life Sci. 74 (2017) 2345–2360.

[42] T. Komai, M. Inoue, K. Morita, T. Okamura, K. Yamamoto, Revisiting the regulatory roles of the TGF-β family of cytokines, Autoimmun. Rev. 15 (2016) 917–922.

[43] J. Myllyharju, K.I. Kivirikko, Collagens, modifying enzymes and their mutations in humans, flies and worms, Trends Genet. 20 (2004) 33–43.

Published in : Matrix Biology (2018), vol. 70, pp. 140–157
DOI: https://doi.org/10.1016/j.matbio.2018.04.002
Status : Postprint (Author's version)

Supplemental data

Adamts2

5'**cagtgccctcgccaagcccaa**ggccatccgacgagcctgcaaccctcaggagtgctcccagcctgtgtgggtc
accggtgaatgggagccttgtactcaaagctgtgggcgaactggcatgcaggtgcgctccgtccgctgtatacaa
cctctgcacaacaacaccacccgctccgtgcacaccaaacactgcaacgatcaccgtcccgagagccgccgggcc
tgcaaccgtgagctctgccctgggcggtggcgggctgggtcctggtcccagtgttcggtaacctgtggcaacggc
acccaggaacggccagtgctctgtcgcactgcagatgataattttggtgtctgccgggaggagcgaccggagacg
gcaaggatctgcaggcttgcaccctgtccccgaaacggctcagatccctccaagaagagctacgtggttcagtgg
ctgtcccggcctgatcctgactcacctatccagaagatctcgtcaaaggaccagtgccaaggcgacaagtcaatg
ttctgtaggatggaagtcttgtctcgctac**tgctccatccccagctacaacaag** 3'

Adamts14

5'tgtgtgaccataaaaagaggcccaagcctatccgacggcgttgcaaccagcactcgtgtccccagcccacgtg
ggtgacagaagagtggggtgcctgtagccgaagctgcgggaagctggggctgcagacccggggagtgcagtgcct
gctgcctctctccaatggcacccacaaagccatgccagccaaggcctgcctaggtaaccggccagaggccaagaa
gccatgcctccgtgtgccctgcccagcccagtggcggacaggagcctggtcccagtgctctgctacctgcggaga
aggcatccagcaaaggcaggtggtatgcaggaacacttccagtgccctcgggccatgcgaaggggtcaagccgga
catggtgcagatctgcagcctgcctgcctgtggaggagatctccagaactctacagtgaaggcggaggtccagga
ccctgtgaccaaaacaggataccgggaaccccaatccaggcccctgactcctgaggacaggatctcaacaatgga
gccctgtgtgcgagacagatccgtcttctgccgaatggaagt**gttggaccgttactgcaccatcc 3'**

Table S1: Sequences used for the generation of probes for "*In Situ* Hybridization". The sequences in bold correspond to the primers used for PCR amplification.

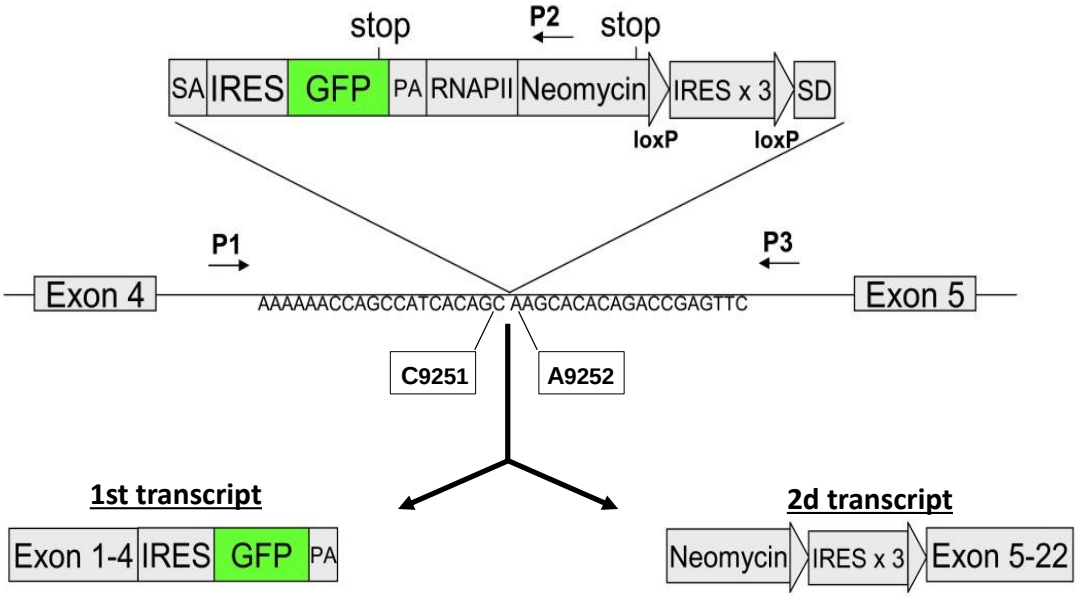

Figure S1: Gene Trap cassette for the generation of Adamts14-deficient mice.
A genetrap cassette was found to be inserted in the "CMHD-Gt_511E11" R1 ES clone between C9251 and A9252 of the intron 4 of the Adamts14 gene. This cassette contained the coding sequence of Green Fluorescent Protein (GFP) flanked by a splice acceptor site (SA) and an Internal Ribosome Entry Site (IRES) allowing the translation of the GFP coding sequence, and by a polyA signal (PA). The inserted cassette contained also the coding sequence for neomycin resistance (Neomycin) under the dependence of a RNA polymerase II promoter (RNAPII) followed by three IRES positioned in the three

Published in : Matrix Biology (2018), vol. 70, pp. 140–157
DOI: https://doi.org/10.1016/j.matbio.2018.04.002
Status : Postprint (Author's version)

reading frames and flanked by two loxP sequences, and by a splice donor site (SD). Insertion of this cassette in the ES genome led to the production of two transcripts, the first one under the dependence of the Adamts14 promoter and the second one driven by the RNAPII promoter. The first part of the first transcript produces a polypeptide encoded by the sequences of Exon 1 to 4 of Adamts14 while the second half, downstream of the IRES, codes for GFP. The second transcript confers resistance to Neomycin and contains the sequence corresponding to Exon 5 to 22 of Adamts14. P1, P2 and P3 are primers used for mice genotyping.

Figure S2: RT-PCR characterization of the transcripts generated from the Adamts14 gene in the skin of WT, TS14$^{+/-}$ and TS14$^{-/-}$ mice. *Primers specific for sequences located in exon 4 (forward) and exon 6 (reverse) allowed the amplification of the wild type allele (WT and TS14$^{+/-}$). No signal is observed in TS14$^{-/-}$ since the sequences of exon 4 and exon 6 are located on two different transcripts (see Fig S1). A GFP specific sequence is amplified only from the cassette (TS14$^{+/-}$ and TS14$^{-/-}$). Primer pairs specific for exon 2 (forward) and exon 3 (reverse) or exon 5 (forward) and exon 7 (reverse) generate RT-PCR products from the WT allele but also from the first (exons 2-3) or the second (exons 5-7) transcript resulting from the activity of the trapping cassette.*

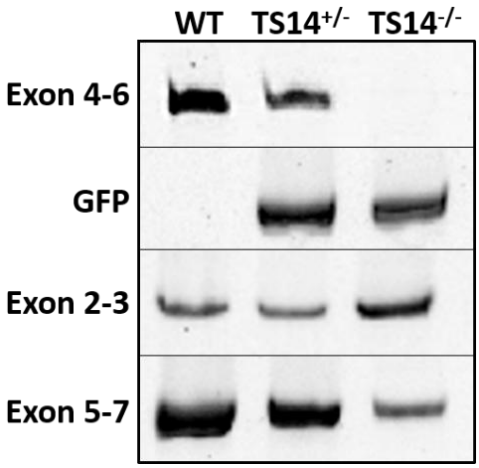

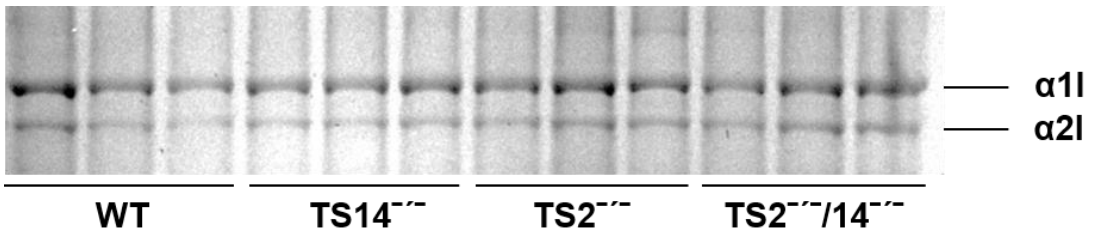

Figure S3: Type I procollagen processing in bone.
Bone samples from three mice of each genotype were decalcified in EDTA for 3 weeks, homogenized and extracted in Laemmli denaturation buffer containing DTT. Proteins corresponding to an identical amount of tissue were submitted to SDS-PAGE and stained (Coomassie blue). For all genotypes, type I collagen appeared as two bands corresponding to the fully processed alpha1 (α1I) and alpha2 (α2I) chains.

Published in : Matrix Biology (2018), vol. 70, pp. 140–157
DOI: https://doi.org/10.1016/j.matbio.2018.04.002
Status : Postprint (Author's version)

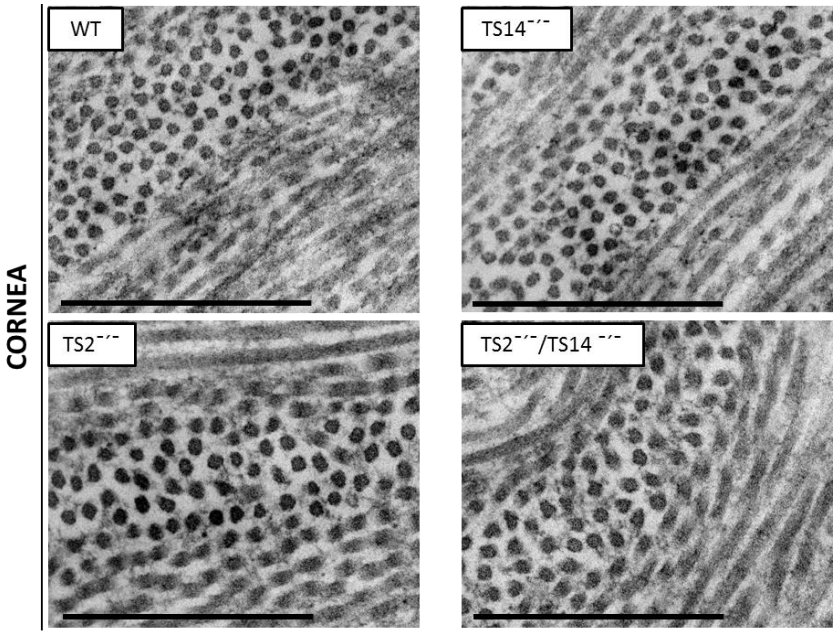

Figure S4: Collagen fibrils in cornea.
Collagen fibrils appear normal and have an identical shape in cornea from the 4 genotypes. (Scale bar = 500nm).

Published in : Matrix Biology (2018), vol. 70, pp. 140–157
DOI: https://doi.org/10.1016/j.matbio.2018.04.002
Status : Postprint (Author's version)

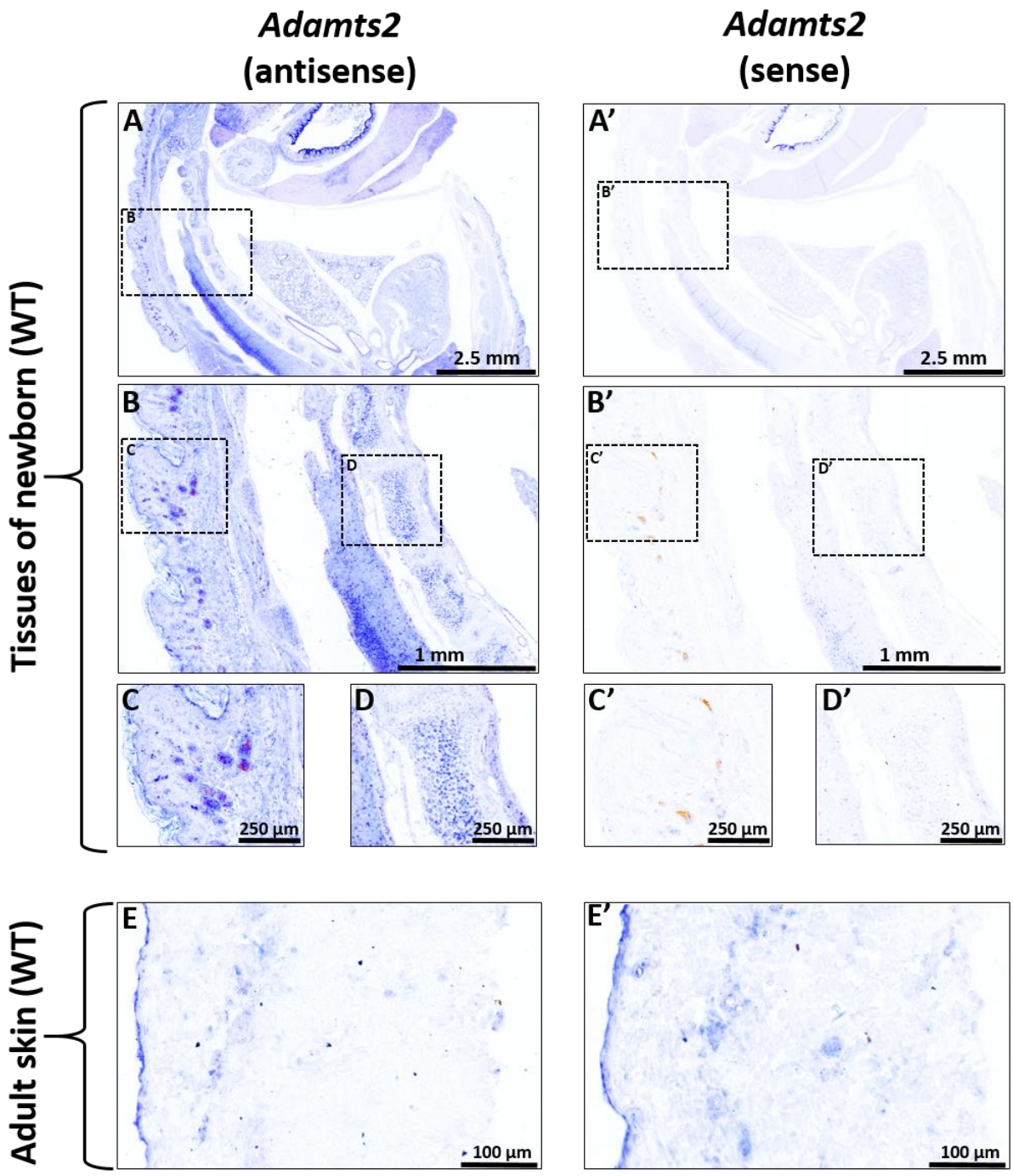

Figure S5: In Situ Hybridization: Adamts2.
Sections of newborns (A-D and A'-D') or of adult skin (E, E') of WT mice were hybridized with antisense (A-E) and sense (A'-E') labeled Adamts2 probes, washed and stained. B (or B') is an enlarged view of the insert in A (or A'). C and D (or C' and D') are enlarged views of B (or B'). Identical revelation times and image acquisition parameters were used for sense and antisense probes. Specific blue staining was observed with the antisense probe on sections of the newborns, especially in vertebrae and in the dermis. In adult skin, the antisense and sense probes gave a low and similar background staining.

Published in : Matrix Biology (2018), vol. 70, pp. 140–157
DOI: https://doi.org/10.1016/j.matbio.2018.04.002
Status : Postprint (Author's version)

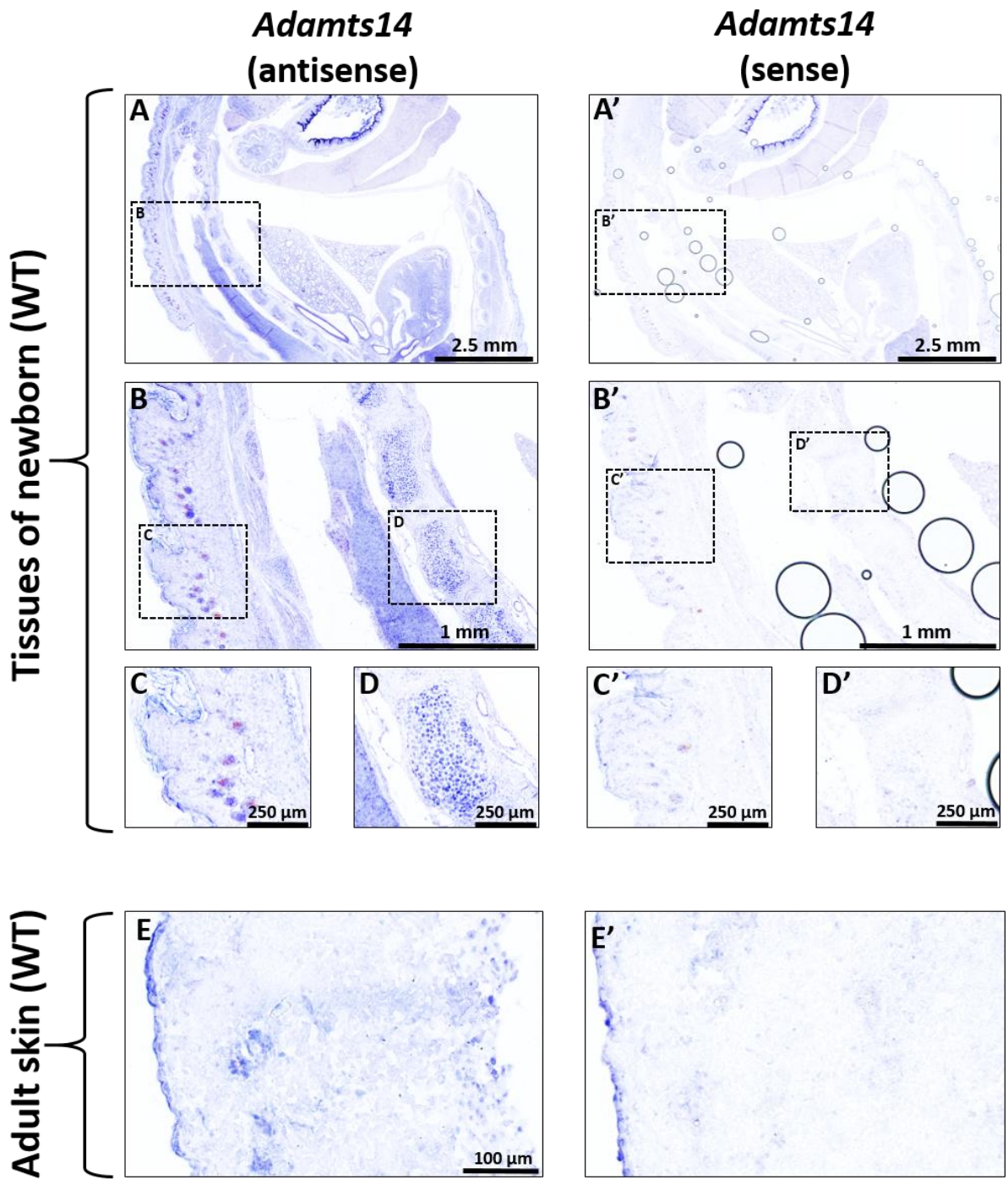

Figure S6: In Situ Hybridization: Adamts14.
Sections of newborns (A-D and A'-D') or of adult skin (E, E') of WT mice were hybridized with antisense (A-E) and sense (A'-E') labeled Adamts14 probes, washed and stained. B (or B') is an enlarged view of the insert in A (or A'). C and D (or C' and D') are enlarged views of B (or B'). Identical revelation times and image acquisition parameters were used for sense and antisense probes. Specific blue staining

Published in : Matrix Biology (2018), vol. 70, pp. 140–157
DOI: https://doi.org/10.1016/j.matbio.2018.04.002
Status : Postprint (Author's version)

was observed with the antisense probe on sections of the newborns, especially in vertebrae and in the dermis. In adult skin, the antisense and sense probes gave a low and similar background staining.

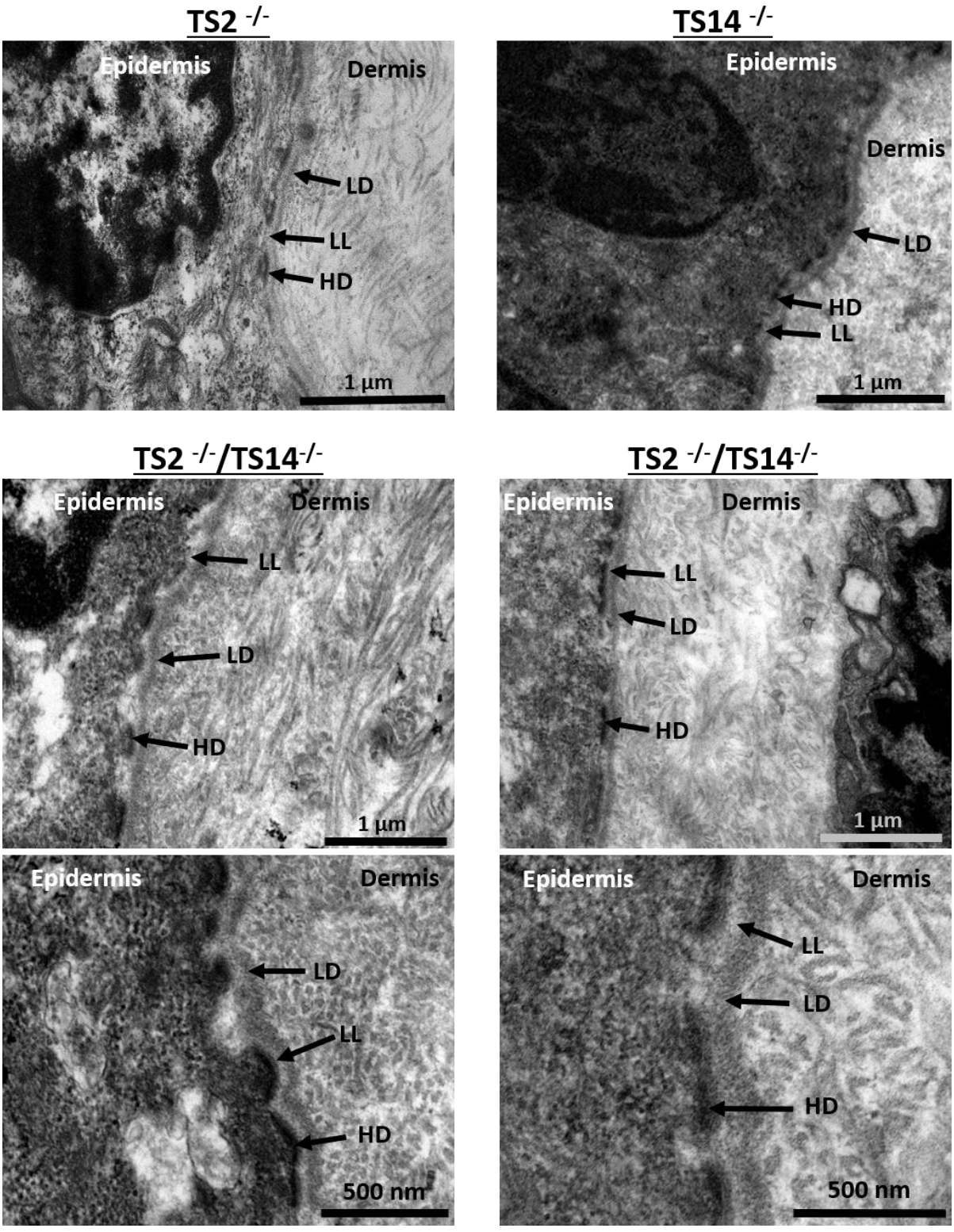

Published in : Matrix Biology (2018), vol. 70, pp. 140–157
DOI: https://doi.org/10.1016/j.matbio.2018.04.002
Status : Postprint (Author's version)

Figure S7: The basement membrane at the dermo-epidermal junction is not altered in TS2$^{-/-}$/TS14$^{-/-}$ mice.

Skin sections were observed by transmission electron microscopy at the junction between the epidermis and the dermis. The structure of the basement membrane in TS2$^{-/-}$/TS14$^{-/-}$ mice is normal and appears as two layers, the Lamina densa (LD) and the Lamina lucida (LL). Its thickness is also normal and similar to that of TS2$^{-/-}$ and TS14$^{-/-}$ mice, and local disruption was never observed. Many hemidesmosomes (HD) anchoring the basal keratinocytes onto the basement membranes are seen in all the samples.

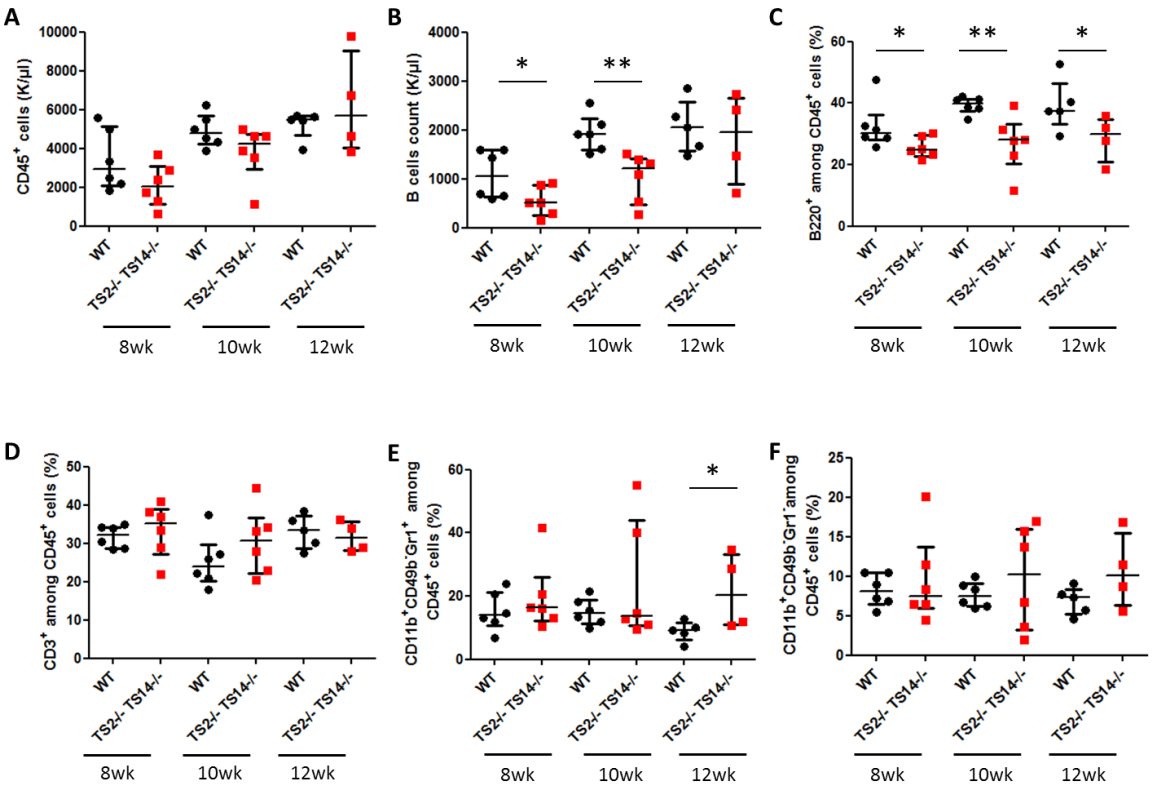

Figure S8: Immune cell profiling in blood of WT and TS2$^{-/-}$/TS14$^{-/-}$ mice at increasing age.

*Blood samples were collected from 6 WT and 6 asymptomatic TS2$^{-/-}$/TS14$^{-/-}$ male mice at the age of 8 weeks. Additional blood samples were also taken 2 and 4 weeks later. Two TS2$^{-/-}$/TS14$^{-/-}$ mice were euthanized at week 11 because lesions appearing during the experiment were too extended. The total number of immune cells (CD45^{+}) (A) and the percentages of T lymphocytes (CD3^{+}) (D), granulocytes (CD11b^{+}CD46b^{-}Gr1^{+}) (E) and monocytes (CD11b^{+}CD49b^{-}Gr1^{-}) (F) were similar for WT and TS2$^{-/-}$/TS14$^{-/-}$ mice at the 3 time points while moderate decreases in B lymphocytes number (B) and proportion (C) were observed. *P<0.05, **P<0.01.*

Published in : Matrix Biology (2018), vol. 70, pp. 140–157
DOI: https://doi.org/10.1016/j.matbio.2018.04.002
Status : Postprint (Author's version)

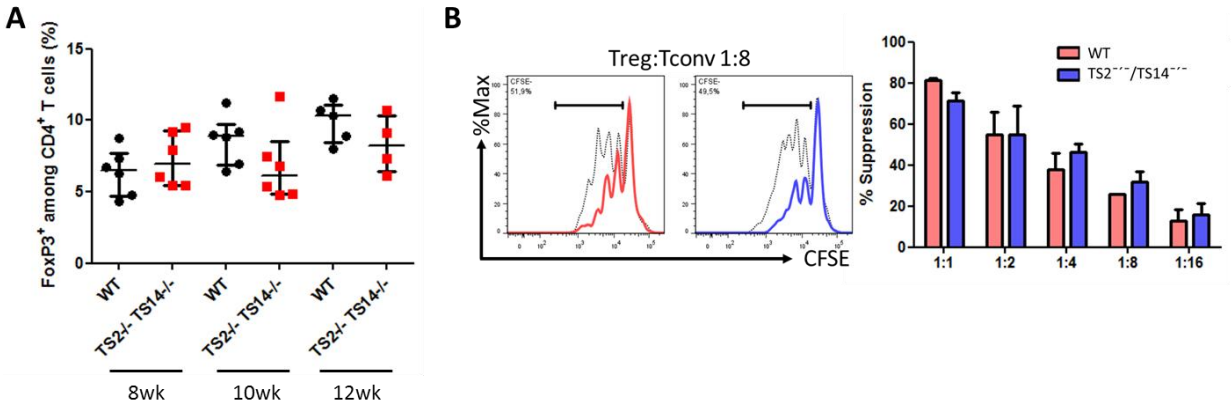

Figure S9: Tregs proportion and function were not altered in blood of TS2$^{-/-}$/TS14$^{-/-}$ mice.
(A) The proportion of Tregs among CD4$^+$ cells (FoxP3$^+$) was measured in the blood of 8, 10 and 12 week-old WT and TS2$^{-/-}$/TS14$^{-/-}$ mice. (B) A functional assay of the activity of Tregs was also performed (CFSE based assay) on Tregs isolated from the spleen of 12 week-old WT and TS2$^{-/-}$/TS14$^{-/-}$ mice. No significant difference was noted between the two groups.

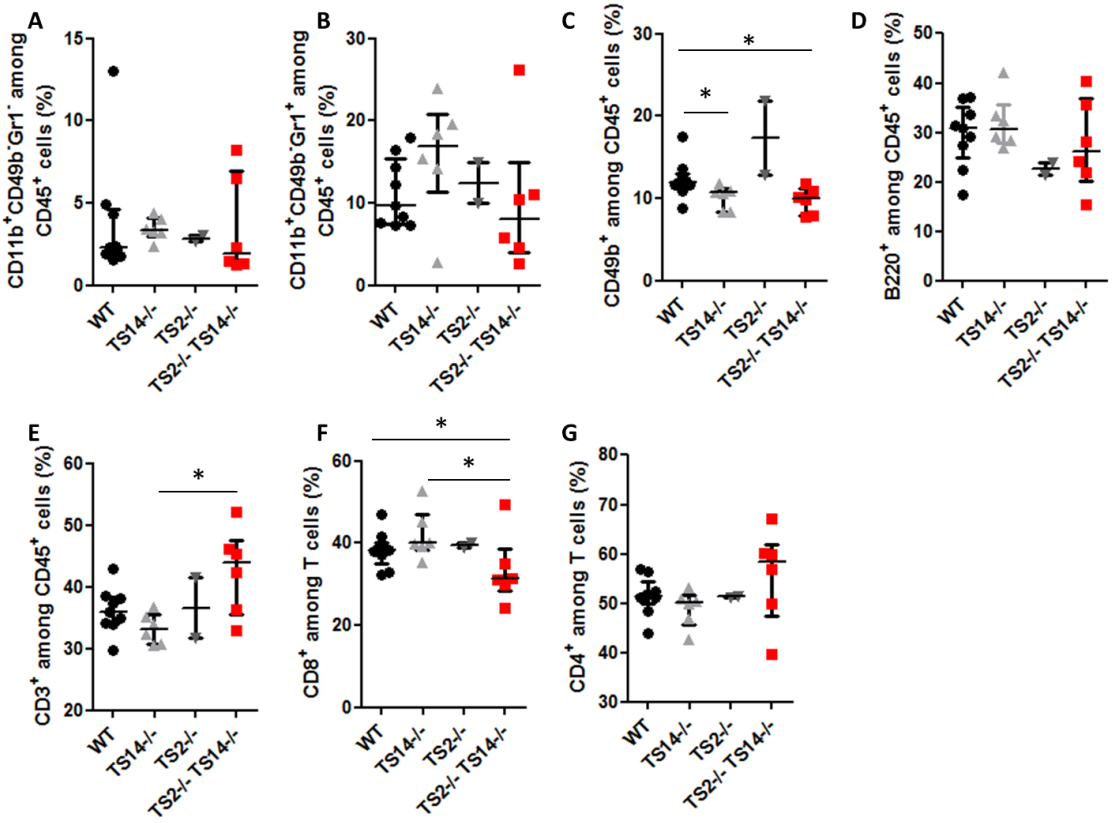

Figure S10: General profile of immune cells in blood from WT, TS14$^{-/-}$, TS2$^{-/-}$ and TS2$^{-/-}$/TS14$^{-/-}$.
*FACS analyses were performed on blood of 8 week-old mice. The profile of monocytes (CD11b$^+$CD49b$^-$Gr1$^-$) (A), granulocytes (CD11b$^+$CD49b$^-$Gr1$^+$) (B) and B lymphocytes (B220$^+$) (D) were similar between the 4 genotypes while a slight reduction of the proportion of NK cells (CD49b$^+$) (C) was observed in TS14$^{-/-}$ and TS2$^{-/-}$/TS14$^{-/-}$ mice. The percentage of T lymphocytes (CD3$^+$) (E) was increased in TS2$^{-/-}$/TS14$^{-/-}$ mice. Modifications of the relative abundance of CD4$^+$ and CD8$^+$ T lymphocytes (F, G) were also observed in TS2$^{-/-}$/TS14$^{-/-}$. *=P<0.05.*